FACULTY OF SCIENCE AND TECHNOLOGY

BACHELOR'S THESIS

Study programme / specialisation: **Energy and Petroleum Technology**	The *spring* semester, *2023* **Open access**
Author: **Jan Christer Åsly & Simon Groven Iversen**	
Supervisor at UiS: **Jan Aage Aasen** Co-supervisor: **Foster Dodzi Gomado** External supervisor(s):	
Thesis title: **Repeated push-out testing of expansive cement plug in casing**	
Credits (ECTS): **20**	
Keywords: **Shear Bond** **Expansion** **Peak Load** **Expansive agent**	Pages: **69** + appendix: **0** **Stavanger, *15th of May 2023***

Repeated push-out testing of expansive cement plug in casing

By
Simon Groven Iversen & Jan Christer Åsly

Bachelor's Thesis

Presented to the Faculty of Science and Technology

University of Stavanger

May 2023

Acknowledgement

We would like to thank our supervisor, Professor Jan Aage Aasen, for helping us through our research, providing us with helpful advice and tips, and giving us this great opportunity. We would also like to show our gratitude to PhD Student Foster Dodzi Gomado for providing directions and help in the lab. We also appreciate Jostein Djuve, Kim Andre Nesse Vorland, and Sivert Bakken Drangeid for providing us with access and necessary training in the laboratory. Finally, we would like to thank our family, friends, and classmates for their good support and encouragement.

The authors acknowledge the Research Council of Norway (RCN) for financing the Centre for Research-based Innovation "SWIPA - Centre for Subsurface Well Integrity, Plugging and Abandonment", RCN project. no. 309646, for which the work has been carried out. The centre is also financed by the operating companies AkerBP, Equinor ASA and Wintershall Dea Norway, and includes in addition more than 20 in-kind contributing industry partners. The R&D partners in SWIPA are SINTEF, NORCE, IFE, NTNU and UiS.

The authors would like to thank the Research Council of Norway (RCN) and NORCE for financially funding the project "#308767 - Fluid migration modeling and treatment project". The authors would also like to thank RCN, TotalEnergies, AkerBP, and ConocoPhillips for their support through the SafeRock project (#319014 - New Cementitious Material for Oil Well Cementing Applications - SafeRock).

Summary

In the petroleum industry, cement plays a crucial role during well operations as it connects the casing pipes to the formation and forms a seal that prevents fluid migration, ensuring well integrity. The ability of the cement to form a strong bond with the formation and casing pipes is an important consideration in designing slurries. In this study, we aimed to investigate whether an expanding cement slurry requires greater force to push compared to a non-expanding slurry. For our experiment we have used two different slurries, namely Neat Class-G with no additives and Halliburton blend containing 5% MicroBond for expansion. We conducted repeated push-out testing on each cement plug at weekly intervals for three weeks, with three independent specimens created for each batch to minimize errors. This experiment enabled us to evaluate the response of the cement plug after experiencing the effect of time and multiple push-out events and subsequently re-establishing bonding with the casing. The push-out testing is used to monitor the shear bond strength, which should be greater than the stress acting on the interface to ensure that the cement sheath remains intact during drilling and production operations.

In addition, we wanted to find a correlation between linear and volumetric expansion. The expansion experiments provide important insights into the push-out testing, as expansion has an impact on the shear bond strength. We performed API-ring testing along with our very own volumetric expansion experiment, to investigate the linear and volumetric expansion. Using these results, we verified a mathematical relationship between them.

Table of content

List of figures

1. Introduction

Cementing is a process that is essential in various industries, from construction and roadwork to oil and gas exploration. But have you ever wondered about the science behind this seemingly simple process?

When we hear the word "cementing," we often think of the gray, powdery substance used in building and construction. But did you know that cementing in the petroleum industry is a vastly different process? It involves pumping a slurry of cement, water, and various additives down the casing and into the annulus between the casing and the formation. The cement slurry then hardens and forms a seal, preventing fluid migration and ensuring well integrity.

The petroleum industry faces unique challenges in cementing, such as high temperature and pressure, corrosive environments, and the need to withstand subsurface stresses. This requires specialized cement formulations and additives to ensure the cement can withstand harsh downhole conditions.

But how do engineers ensure that the cementing operation is successful? What challenges do they face, and how do they overcome them? These are just a few of the questions we explored as we looked closer into cement operations in the petroleum industry.

In this thesis, we delved deeper into the fascinating world of cementing in the world of petroleum, exploring the challenges and advancements in technology that have allowed for safer and more efficient well construction. Several factors come into play when it comes to ensuring that the cement is set and adhered to the casing and formation as it should. One of these factors is shear bond strength - the strength of the bond between the cement and the casing or formation. If this bond strength is too weak, it can lead to costly well failures, environmental damage, and safety hazards. So, how do engineers ensure that the bond strength is sufficient?

They achieve this through various tests. To test the shear bond strength, engineers and scientists use a technique called push-out testing, which involves applying a force to a cement-casing or cement-formation sample and measuring the force required to break the bond. We performed this type of test, and our goal was to see the difference in shear bond strength with and without expansive agents. Is a greater load needed to push the cement with expansive agents? And is the possible difference the same when pushing the cement plug back again, or is the relation different? Another aspect of our experiment is that we did repeated push-out testing, where the same sample is tested every week for three weeks. The goal of doing the repeated push-out testing was to see the effect time and repeated pushing had on the shear bond. The capacity to re-establish bonding following the breakage of initial bonding from an applied force, is also an interesting aspect. Is the cement capable of attaining an equivalent level of shear bond quality after experiencing one, or even two push-out tests?

In addition to shear bond strength, we also were interested in measuring the expansion of the cement - how much it expands after it is set. The API (American Petroleum Institute) ring test is a widely used method for measuring linear expansion and we are also excited to introduce our very own experiment for measuring the volumetric expansion. We wanted to look at the two measured values and find the correlation between them. This helped us decide to which extent our new experiment is usable.

By understanding both the shear bond strength and volumetric expansion of the cement, we can better ensure that the cementing operation is successful and that the well is safe and productive. And thus complete a critical step in the drilling and completion process. So come along for the ride – it is sure to be an intriguing one.

2. Literature review

2.1 Cement

Cement, per definition, is a mineral binder that, when mixed with water, hardens into an extremely hard mass, even underwater. It is differing from slaked lime because it hardens without needing CO_2 from the air. Cement is one of the most used materials in the construction industry. It can be mixed with water, sand, and gravel to make concrete, or with water and sand to make mortar. Both materials can be seen almost everywhere in society. We see it in buildings, roads, bridges, dams, and more.

The most used cement is Portland cement. It was manufactured for the first time in 1824 by Joseph Aspdin. According to Store Norske Leksikon "Portland cement is produced by finely grinding and carefully blending raw materials containing calcium, silicon dioxide, aluminum oxide, and iron oxide (such as limestone or marl, mixed with other materials like clay, shale, sandstone, feldspar, quartz, and similar materials). These materials are burned to incipient fusion (sintering, 1400-1500°C) in rotating kilns, and then finely ground to a powder in ball or tube mills with the addition of approximately 3-5% gypsum and possibly small amounts of iron sulfate and hydraulic active materials, such as fly ash" (Årtun, 2023).

At this point, additives can be put into the cement mix to enhance and change the properties of the cement, but we will dive deeper into these later.

2.2 Cement in the petroleum industry

Cement is used in a variety of ways in the petroleum industry. It is vital in all phases of a petroleum well, including drilling, production, and abandonment. Depending on the reservoir and other aspects, the perfect cement varies, and it is not at all one certain recipe. Factors that decide this can be formation type, temperature, and pressure. Therefore, lots of additives and cement mixes have been made, and new ones are continuously being developed. This is to ensure that we get the optimal mix for every situation. Two principal operations make up well cementing: primary cementing and remedial cementing. Primary cementing is the process of placing a cement sheath between the annulus and the formation. Remedial cementing is when you need to do an additional cementing job after primary cementing. This can for example be because the primary cementing job failed or because the well is going to be abandoned.

2.3 Primary cementing

The primary cementing operation objective is to clear the casing interior and borehole of drilling fluid, place a cement slurry in the annulus, and fill the casing interior with a displacement fluid such as brine, water or drilling fluid. This is to achieve zonal isolation, in addition to supporting and anchoring the casing string in addition to protecting the casing from corrosion. The reason for not mixing cement and drilling fluid, is that these two generally are incompatible chemically. If mixed, they can form a thick gel that will be hard to remove. This can result in a cement sheath that is not uniform in the annulus. One of the ways to keep them from mixing is to use chemical washers and spacer fluids. These are pumped after drilling fluid and before the cement to ensure that they are kept separated. In addition, chemical washers and spacer fluids may benefit the cement bonding by cleaning both the casing and the formation.

There are a few different methods for primary cementing, but the most used is a two-plug cement placement method shown below in Figure 1. First, an interval of a set desired depth is drilled, before the drill pipe is removed. At this point, only drilling fluid remains in the borehole. Then a casing string is lowered to the bottom, with a guide shoe or float shoe at the end. These devices are used to guide the casing into the center of the borehole in cooperation with centralizers which are placed at weak or critical points of the casing. The reason for trying to keep it in the center is to prevent casing from sticking, avoid rough edges or washouts and place a uniform sheath of cement in the annulus.

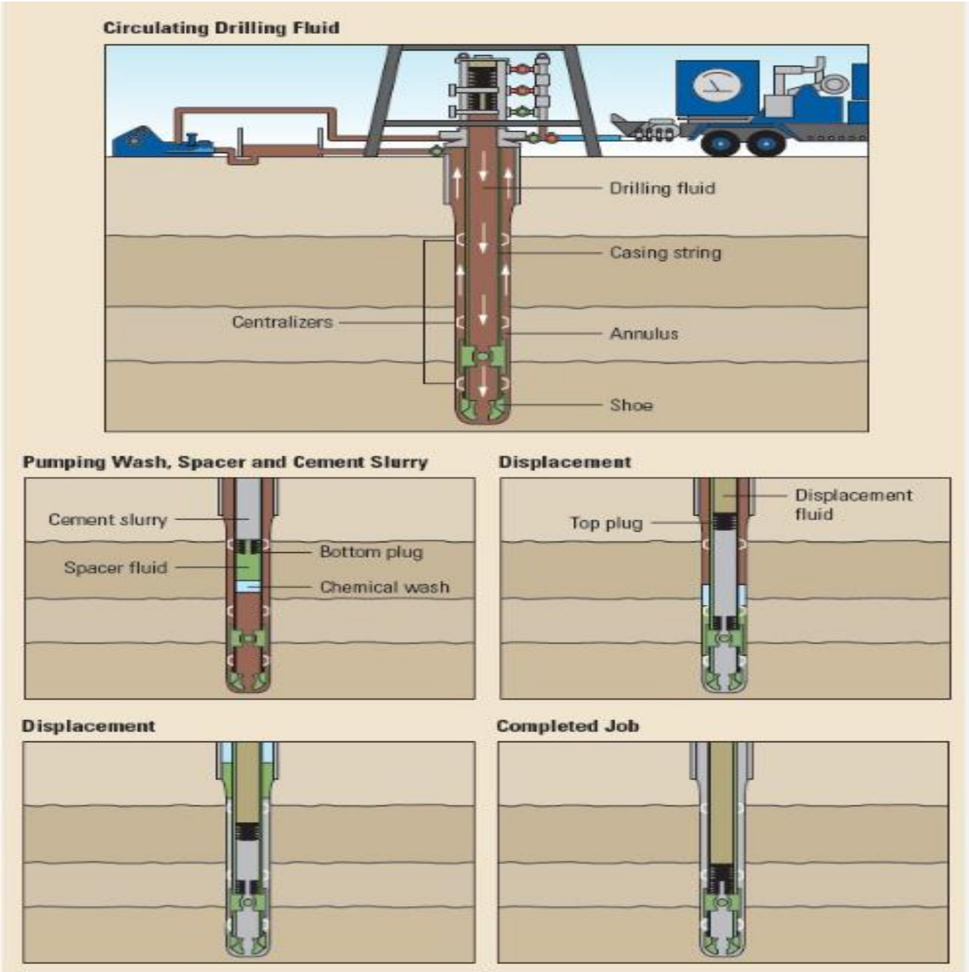

Figure 1: Drilling operation

Wiper plugs act as a physical barrier separating the fluids inside the casing. The bottom plug divides the cement slurry from the drilling fluid, and the top plug separates the cement slurry from the displacement fluid. Once the bottom plug lands at the bottom of the casing string, its membrane ruptures to form a pathway through which the cement slurry flows into the annulus. The top plug does not have a membrane; therefore, when it rests on top of the bottom plug, the hydraulic communication between the casing interior and the annulus is cut off. Following the cementing process, engineers must wait for the cement to cure, set and develop strength, which is commonly referred to as *waiting on cement*. After the waiting on cement period, which typically lasts less than 24 hours, additional drilling, perforating or other operations may proceed.

Normally the well is so deep that multiple casing strings need to be placed. Each casing string is smaller in diameter than the last as you go down the well. All these casing strings need their own Primary cementing operation. In a typical casing program, there are four types of casing being cemented inside the well. All types with their respective names are shown in Figure 2.

First, a large diameter *Conductor casing* is put into the top of the well to protect the shallow formations from contamination as well as preventing washouts. Afterward, a *Surface casing* is put inside the Conductor casing and cemented.

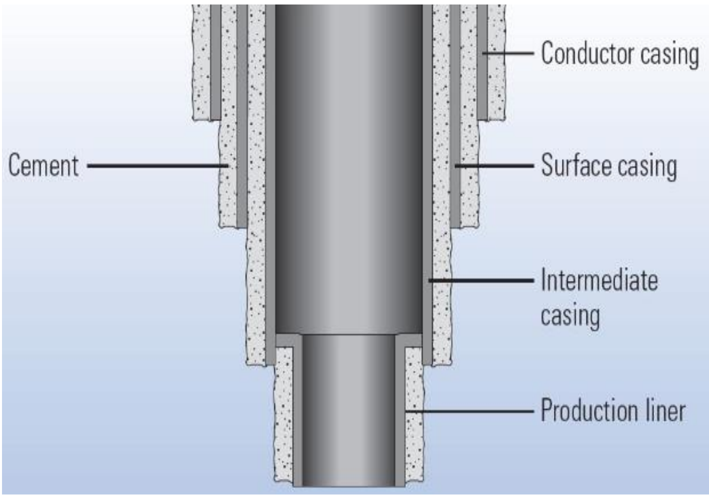

Figure 2: Cement operation

The objective of the surface casing is to preserve the integrity of the wellbore and ensure that shallow groundwater is protected from contamination by drilling fluids and hydrocarbons. Next is the *Intermediate casing,* which serves as a barrier that isolates hydrocarbon-bearing, abnormally pressured, fractured, and lost circulation zones, that way ensuring well control as drilling operations progress to greater depths. Depending on the target production zone, multiple intermediate casing strings may be needed to reach the required depth. Lastly, the casing with the smallest diameter is the production casing. Production casing is also commonly referred to as liner. The objective of the liner is to isolate all zones within the production zone, as well as all the zones above it. The liner also needs to be able to withstand all the expected loads during the well lifetime. Failure to achieve any of these casing objectives may severely limit the well's ability to reach its full producing potential and may have severe consequences.

2.4 Remedial cementing

If the *Primary cementing* job has failed, a *Remedial cementing* operation can be the answer. Remedial cementing can help in all parts of a well lifecycle, from drilling to production and all the way to abandonment. These processes are divided into two groups: Squeeze and Plug cementing. There are some differences in when and where they are used, but they also share some uses. Both are helpful when dealing with lost circulation zones depending on the situation. Plug cementing is, among other things, beneficial when you need to initiate directional drilling or to sidetrack around debris. Squeeze cementing is for example used to repair faulty primary cementing or to eliminate water intrusion in the production zone. Some remedial cementing methods are shown in Figure 3.

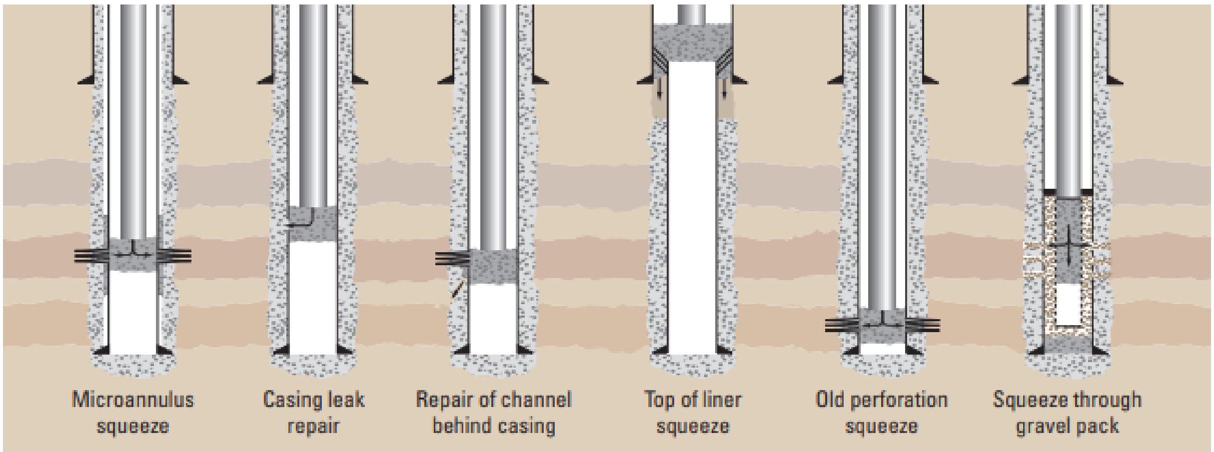

Figure 3: Cement operation 2

During *squeeze cementing,* a cement slurry is forced through holes and fissures in the casing/wellbore annular space. One example of squeeze cementing is sealing leaks in annular space before abandoning a well. The way squeeze cementing works is that when the slurry is forced into the formation, the solid particles will create a filter cake on the formation while the aqueous phase goes into the formation. The excess cement slurry inside the wellbore will be washed away in the cleaning phase. If the operation is successful, the filter cake will close the opening and set to become an impermeable solid.

A *plug cementing* process is when a smaller volume of cement slurry is placed into the wellbore and allowed to set to create a solid plug. There are different ways to do this, and the most used method is the *balanced plug*. To complete the procedure, drill pipe or tubing must be inserted into the wellbore until the plug base is reached. A proper volume of spacer or chemical wash is pumped both before and after the cement slurry to prevent mud from polluting the region. The volumes are carefully calibrated to ensure that they reach identical heights in the annulus and pipe.

2.5 Additives:

Additives can help us in many ways in perfecting our cement. As previously mentioned, there are many different problems to encounter, and there is no set answer. Therefore, we have lots of different types of additives that change the cement's properties. Nelson and Gulliot state in their book *Well Cementing* that we have the following eight types of additives with different functions (Guillot and Nelson, 2006):

- *Weighting agents* that increase the density of the cement slurry
- *Extenders* that lower the density of the cement slurry and or reduce the quantity of cement per unit volume of product.
- *Accelerators* that reduce the setting time of the cement slurry and increase the rate of compressive strength development.
- *Retarders* that delay the setting time of the cement slurry.
- *Dispersants* that reduce the viscosity of the cement slurry.
- *Fluid-loss control agents* that control leakage from the aqueous phase of the cement system to the formation.
- *Lost-circulation control agents* that control the loss of the cement slurry itself to formations.
- *Specialty additives* with different functions.

In this thesis, we will be using an expansive agent named MicroBond. Expansive agents can help to compensate for the shrinkage of the cement as it sets, which can cause voids or gaps to form between the cement and the surrounding formation. This is particularly important in oil and gas wells, where any gaps can create pathways for fluids to migrate between different formations or zones, potentially causing problems such as water or gas breakthroughs.

Secondly, the expansive agent can help to improve the bond between the cement and the surrounding formation, which is important for maintaining the integrity of the well. This is because the expansion of the cement can help press tightly against the formation, increasing the contact area and improving the shear bond strength.

Expansive agents work by generating gas bubbles or crystals during hydration, which create pressure and contribute to an increase in volume. There are different types of expansive agents, but one common example is calcium sulfoaluminate (CSA). When CSA reacts with water, it forms ettringite crystals that take up more space than the initial components. This reaction generates an expansive force that counteracts the shrinkage of the cement, leading to a net increase in volume. The effectiveness of expansive agents depends on factors such as the type and amount of additive, as well as the conditions during placement and curing. In some cases, excessive expansion can lead to cracking or other issues, so careful selection and testing of additives are essential to ensure optimal performance.

In this thesis, we are going to have a closer look at the difference MicroBond gives in shear bond strength during the push-out testing. As mentioned, we are particularly interested in seeing if the cement with an expansive agent requires a greater push-out load to move the plug than the Neat-G cement, and if the difference is the same for pushing it one way and when pushing it back again.

2.6 Bonding / Shear bond

There are several forms of interfacial bond strength, including tensile, shear, and hydraulic strengths. Tensile bond strength is characterized by the amount of resistance that the interface presents against perpendicular tensile loads necessary for its separation. Shear bond strength, on the other hand, is the strength required to initiate failure in parallel to the load direction. Lastly, hydraulic bond strength works against fracture propagation along the bonded interface, induced by excessive fluid pressure. Hydraulic bond is most important for zonal isolation. Shear bond gives mechanical support to the drill pipe in addition to zonal isolation and is a measurement of how much force is needed to initiate movement, divided by contact area.

In the push-out testing, we are monitoring the shear bond strength. The shear strength of the cement sheath should be greater than the stress acting on the interface to ensure that it remains intact during drilling and production operations. A strong shear bond between the cement sheath and the casing or formation prevents annular fluid migration and gas or water intrusion, which could compromise the well integrity. The cement slurry properties, such as its density, viscosity, and setting time, can influence the shear bonding strength of the cement sheath. Optimizing the cement slurry design and placement is crucial to achieving strong shear bonding and ensuring effective zonal isolation in petroleum wells.

A weak bond between the cement and the wellbore can lead to a lack of zonal isolation, where fluids are able to migrate between different zones in the well. This can cause a range of problems, including reduced well-productivity, the risk of cross-contamination between different formations, and even well-blowouts. In addition, a weak bond can also lead to a lack of mechanical support for the casing, which can result in casing collapse or damage. Overall, a low shear bond strength in petroleum cementing can have serious safety and economic implications for the well-operation. It is therefore critical to ensure that the bond strength meets industry standards and best practices.

3. Preparation of experiments

The thesis will comprise three distinct experiments, with a primary focus on push-out testing. Repeated push out testing was conducted on each cement plug once every week for three weeks. In addition, two supplementary experiments were conducted to improve our comprehension of the cement's behaviour. An API ring test was performed to determine the cement's linear expansion or shrinkage, while the final experiment involved bulk expansion testing to investigate the cement's external volumetric changes. To maintain consistency across all experiments, identical recipes and mixing techniques were utilized, according to established standards.

3.1 Preparation of slurry

In our experiment we used two different cement slurries, Neat-G and Halliburton blend. The Neat-G slurry will sometimes get referred to as ''Batch 1'' while the Halliburton blend is sometimes referred to as ''Batch 2''. We completed the test using three independent specimens of each slurry, to have a wider range of test results. By doing this we decreased the possibility of errors.

3.2 Recipe

Neat Class-G

Material	Weight	Mixing time	Total volume
Cement: Dyckerhoff Class-G	792 g	15 + 35 s	
Water	348 g	15 + 35 s	
Additions	None	None	
			600 ml

Table 1: Recipe Neat Class-G

Halliburton Blend (expanding)

Material	Weight	Mixing time	Total volume
Cement: Dyckerhoff Class-G	792 g	15 + 35 s	
Water	348 g	15 + 35 s	
Additions: MicroBond (5%)	39,6 g	15 + 35 s	
			600 ml

Table 2: Halliburton Blend

Dyckerhoff Class-G is a basic oil well cement and is one of the special hydraulic binding materials. The main content of the cement comes from Portland cement, which is the most common type of cement in general use around the world. There are several types of Portland cement available with small variations depending on the purpose of the cement. This type of cement was developed early in the 19th century in England. The basic ingredients are limestone, shells, chalk/marl combined with clay, slate, blast furnace slag, silicia sand and iron. These ingredients go through a drying method, starting by crushing and mixing the stone materials. Before getting heated to about 2700 degrees Fahrenheit before getting burned and grinding and mixing it with small amounts of gypsum. These are only the main steps of the process and can vary, but for us it is not necessary to go in deeper into the details of it.

The Class-G cement is also known as block cement or blockage cement. To get to know this type of cement and better understand why it is used in oil wells we need to look at its characteristics. With ideal density and setting time it has lower consistency and a good resistance to sedimentation. It has good pumpability and when pre-mixing the cement we can inject the concrete to the target position in the oil well. It can have a rapid setting time and strong mechanical strength. It also has good impermeability, stability, and corrosion resistance. We will only be using one additive, the MicroBond, which makes the cement expand more than the neat mix. There are many different additives that can be used for different purposes. This gives many opportunities to optimize the slurry for each situation and fulfil demands.

For the Neat Class-G mix we used 44% water of the mass fraction of cement. There are API standards which the cement must fulfill, but mostly it has a quite good margin towards these standards. Maximum MgO% and SO3% must be less than 6% and 3%, but most often it is around 0,9% for the MgO and 2,7% for the SO3. The free fluid must be less than 5,9%, but most of the time it is approximately 1,9%. The quantity of tricalcium silicate (C3S) must be between 48 and 65 percent, and for the tricalcium aluminate (C3A) it must be less than 3%.

The density of the slurry should be around 1,91 kg/l and absolute grain density 3,18 g/cm^3. While the compressive strength 8h/38°C must be higher than 300 psi and 8h/60°C higher than 1500 psi. Thickening time (time to 100 Bc) should be between 90 and 120 min. (Dyckerhoff, 2021)

The MicroBond is an additive that promotes crystalline growth at low temperatures, but instead of causing contraction, it results in expansion. It includes a combination of essential components that facilitate low-temperature expansion, and it is compatible with all types of Portland cement.

3.3 Mixing

Test samples were prepared in accordance with ISO 10426-2. We used a Waring blender which has an automatic blending setting, with API recommended speed. This setting consists of a total of 50 seconds, using 4000 rpm for 15 seconds and 12000 rpm for 35 seconds. The dry phase was added to the water during the first 15 seconds.

To avoid materials being caught in the walls of the mixing cup we used a spatula to push it down in the mix during the 35 seconds mixing period.

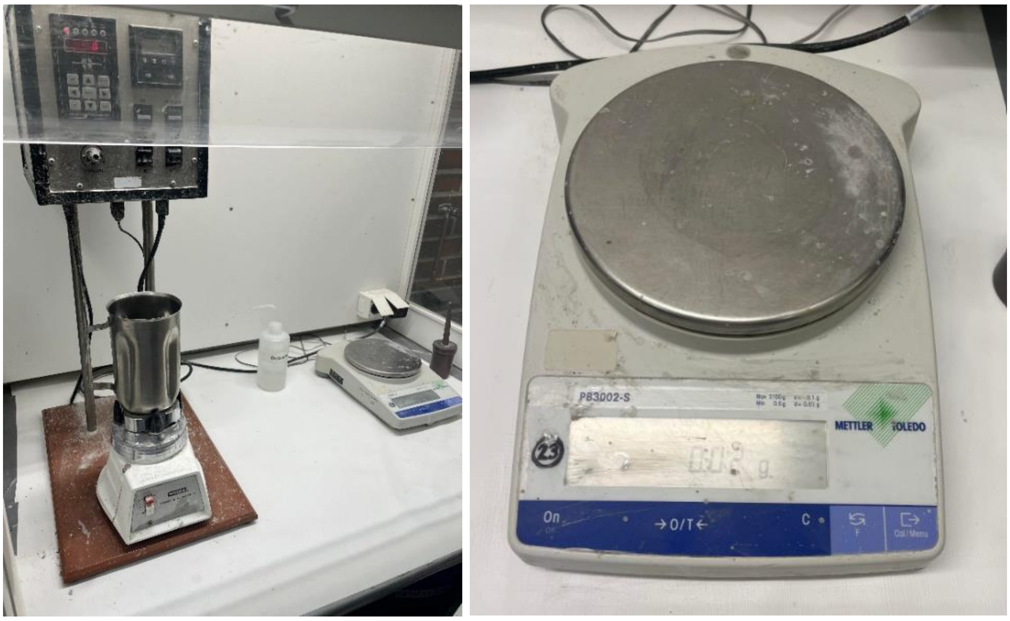

Figure 4: Waring blender and Mettler scale

4. API ring testing

By doing this test we wanted to discover the linear expansion or shrinkage of the cement slurries. We did one batch with Neat Class-G and one batch with Halliburton blend which has the expansive agent MicroBond added to it.

Linear expansion is the phenomenon of an object increasing in length due to a change in temperature. When an object is heated, its atoms and molecules start moving more rapidly, and this causes them to spread out and occupy more space. This increased motion causes the object to expand in all directions, but in the case of linear expansion, the expansion is mostly confined to one direction, usually the length of the object. Like most materials, cement also exhibits linear expansion when it is subjected to a change in temperature. When the cement sets and hardens, it undergoes a process called hydration, which generates heat. In summary, linear expansion is a property of cement that describes its tendency to expand or contract in response to a change in temperature. Engineers must take this property into account when designing slurries to avoid unwanted behaviour inside the well.

4.1 API ring

We did this experiment according to ISO 10426, which provides the methods of testing well cement. By following this method, we were able to determine the dimension changes during the curing process. This method takes place under atmospheric pressure only, so we needed to have in mind that real well cementing happens under high pressure and different boundary conditions.

The method uses an API ring to do the tests, which is standard equipment designed for this purpose.

Figure 5: API Ring

The API ring has the following requirements for the standard size of the ring: The outer diameter (OD) of the inner ring shall be 50,8 mm (2 in), and the inner diameter (ID) of the outer expansion ring shall be 88,9 mm (3,5 in).

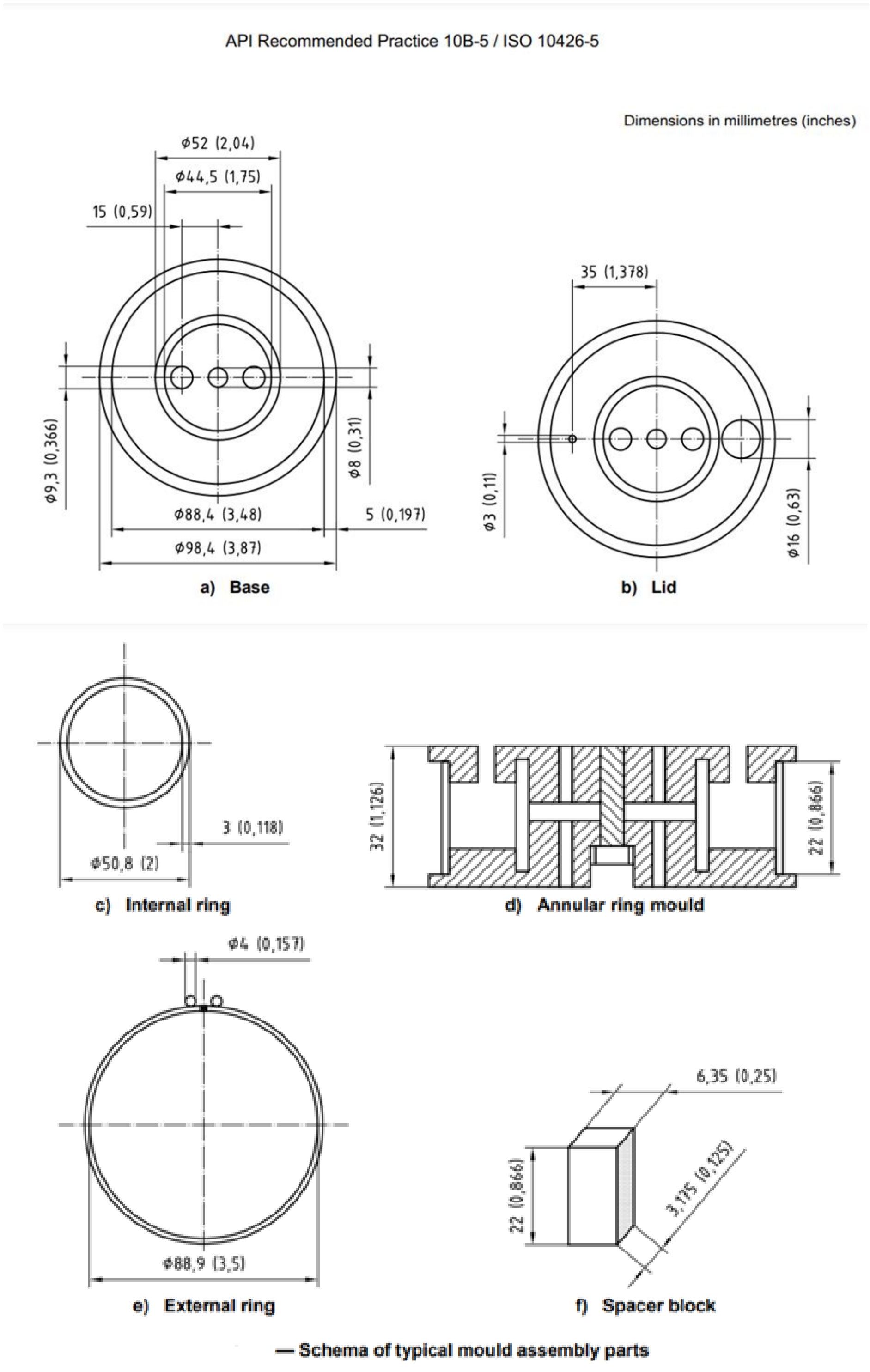

Figure 6: API Ring standards sizes

4.2 Procedure

The slurry gets poured into the large fill hole of the outer portion of the API ring, until the slurry exits the small hole. The ring is then placed in a water bath that holds 25 degrees Celsius. Here we leave it for seven days to cure. The expansion/shrinkage gets measured after 24 hours, 72 hours and at last after the seven days has been completed. For the measuring we will be using a micrometer, in addition we also must take a measurement immediately after pouring the slurry. By doing this, we know what our starting distance is and we can see how it varies over the time period. The micrometer is placed outside the two steel balls attached to each side of the split in the expandable ring. The measuring should be taken less than five minutes after removing it from the curing bath. The micrometer has a precision of 0,02 mm.

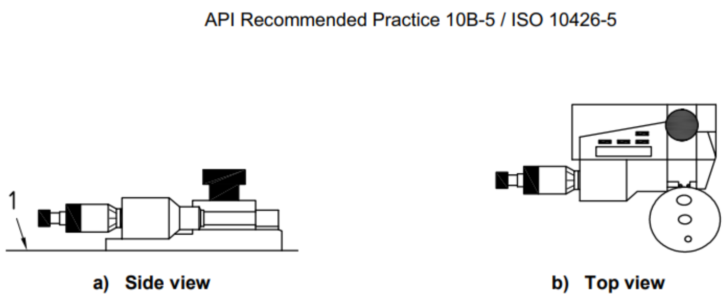

Figure 7: Micrometer standard

Figure 8: Micrometer

Figure 9: Curing bath

4.3 Formula

Standard SI formula to determine the percent circumferential change (shrinkage or expansion).

Equation (1);

$$\boldsymbol{l}_{\Delta,\boldsymbol{SI}} = \left(\boldsymbol{l}_{\boldsymbol{f},\boldsymbol{SI}} - \boldsymbol{l}_{\boldsymbol{i},\boldsymbol{SI}}\right) x \ 0{,}358$$

Equation 1: Percent circumferential change

Where;

$\boldsymbol{l}_{\Delta,\boldsymbol{SI}}$ = Percentage circumferential change of the cement sample.

$\boldsymbol{l}_{\boldsymbol{f},\boldsymbol{SI}}$ = The distance after curing, expressed in mm.

$\boldsymbol{l}_{\boldsymbol{i},\boldsymbol{SI}}$ = The initial distance before curing.

The constant factor 0,358 is obtained from the two following equations;'

Equation (2);

$$\text{Circumferential of circle} = \pi \text{ x } \mathbf{d}$$

In the API standard they have used a diameter of 88,9 mm which gives us →

π x 88,9mm = 279, 288 mm.

Equation 2: Circumferential of circle

In order to use this in form of percent we put it in equation (3);

$$\frac{100\%}{279{,}288\ mm} = 0{,}358\ \%\ per\ mm\ changed$$

Equation 3: Percent change per mm change in API-ring

This is the derived formula we will be using to analyse our results from the API-ring testing.

4.4 Results API ring testing

4.4.1 Neat Class-G:

Specimen 1:

Time	Measured distance	Expansion
01.02.23 – 11:15	11.888 mm	0
02.02.23 – 11:15 (24 hours)	12.438 mm	0.550 mm
04.02.23 – 11:15 (72 hours)	12.436 mm	- 0.002 mm
08.02.23 – 11:15 (168 hours)	12.413 mm	- 0.013 mm
Total		0.525 mm

Table 3: Result Neat Class-G specimen 1

Total expansion for specimen 1, in percent;

$$\boldsymbol{l}_{\Delta,\boldsymbol{SI}} = \left(\boldsymbol{l}_{\boldsymbol{f},\boldsymbol{SI}} - \boldsymbol{l}_{\boldsymbol{i},\boldsymbol{SI}}\right)\ x\ 0{,}358 = (12{,}413\ mm - 11{,}888\ mm)\ x\ 0{,}358 = 0{,}188\ \%\ change$$

Specimen 2:

Time	Measured distance	Expansion
08.02.23 – 13:00	11.880 mm	0
09.02.23 – 13:00 (24 hours)	12.247 mm	0.367 mm
11.02.23 – 13:00 (72 hours)	12.260 mm	0.013 mm
15.02.23 – 13:00 (168 hours)	12.286 mm	0.026 mm
Total		0.406 mm

Table 4: Result Neat Class-G specimen 2

Total expansion for specimen 2, in percent;

$$\boldsymbol{l}_{\Delta,\boldsymbol{SI}} = \left(\boldsymbol{l}_{\boldsymbol{f},\boldsymbol{SI}} - \boldsymbol{l}_{\boldsymbol{i},\boldsymbol{SI}}\right) x\ 0{,}358 = (12{,}286\ mm - 11{,}880\ mm)\ x\ 0{,}358 = 0{,}145\ \%\ change$$

Specimen 3:

Time	Measured distance	Expansion
16.02.23 – 14:00	11.866 mm	0
17.02.23 – 14:00 (24 hours)	12.298 mm	0.432 mm
19.02.23 – 14:00 (72 hours)	12.331 mm	0.033 mm
23.02.23 – 14:00 (168 hours)	12.362 mm	0.031 mm
Total		0.496 mm

Table 5: Result Neat Class-G specimen 3

Total expansion for specimen 3, in percent;

$$\boldsymbol{l}_{\Delta,\boldsymbol{SI}} = \left(\boldsymbol{l}_{\boldsymbol{f},\boldsymbol{SI}} - \boldsymbol{l}_{\boldsymbol{i},\boldsymbol{SI}}\right) x\ 0{,}358 = (12{,}362\ mm - 11{,}866\ mm)\ x\ 0{,}358 = 0{,}178\ \%\ change$$

Neat Class-G graphs:

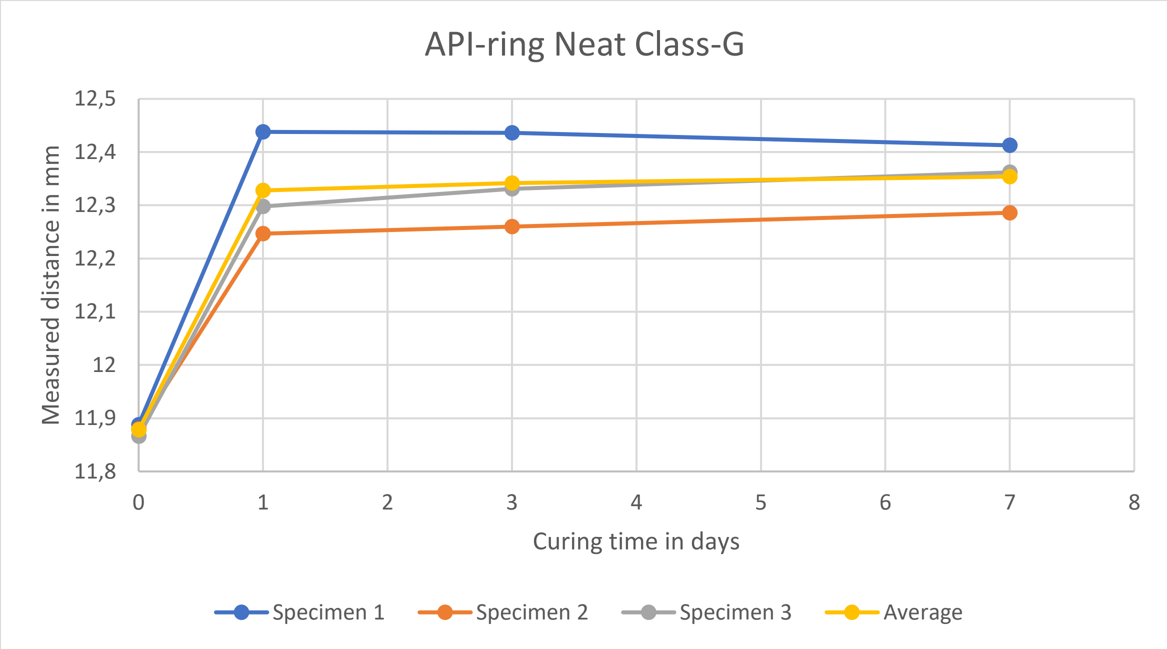

Figure 10: API-ring Neat Class-G graphs

The setting of cement is a complex chemical reaction that involves the hydration of Portland cement. During hydration, water is added to the cement particles, resulting in the formation of calcium silicate hydrate (C-S-H) and calcium hydroxide (CH). This process also results in the generation of heat, which can cause the cement to shrink if it is not properly restrained.

When our cement is allowed to set under water at atmospheric pressure and normal temperature, there is no significant shrinkage because the hydration process occurs at a rate that allows for release of heat generated and there is water around the cement to maintain a constant moisture level. Additionally, it is not exposed to air, and therefore evaporation is minimized.

However, inside the wellbore, the cement slurry is often subjected to high pressures and temperatures and changes in both, which can lead to shrinkage if proper measures are not taken. The shrinkage can be due to thermal expansion and contraction, evaporation or undesirable hydration process. In these conditions, expansive additives, such as MicroBond, can be added to the cement slurry to counteract the shrinkage caused. These additives work by leading to formation of crystals such as CaOH and MgOH, which compensate for the shrinkage. The volume of crystals is typically larger than the combined volume of the components that form them, this way the internal pressure exerted under crystallization causes expansion (Guillot & Nelson, 2006).

In conclusion our cement does not shrink when allowed to set at atmospheric pressure and normal temperature because the hydration process occurs at a rate that allows for the release of heat generated without significant shrinkage, and sufficient restraint is provided to prevent the cement from shrinking. Also, our cement is placed in atmospheric pressure under water, it is fully submerged, and the water can help to maintain the hydration process and prevent shrinkage.

4.4.2 Halliburton blend:

Specimen 1:

Time	Measured distance	Expansion
23.02.23 – 13:30	11.838 mm	0 mm
24.02.23 – 13:00 (24 hours)	12.267 mm	0.429 mm
26.02.23 – 13:00 (72 hours)	12.387 mm	0.120 mm
02.03.23 – 13:00 (168 hours)	12.495 mm	0.108 mm
Total		0.657 mm

Table 6: Result Halliburton blend specimen 1

Total expansion for specimen 1, in percent;

$$\boldsymbol{l}_{\Delta,\boldsymbol{SI}} = (\boldsymbol{l}_{\boldsymbol{f},\boldsymbol{SI}} - \boldsymbol{l}_{\boldsymbol{i},\boldsymbol{SI}})\ x\ 0{,}358 = (12{,}495\ mm - 11{,}838\ mm)\ x\ 0{,}358 = 0{,}235\ \%\ change$$

Specimen 2:

Time	Measured distance	Expansion
02.03.23 – 12:30	11.844 mm	0 mm
03.03.23 – 12:30 (24 hours)	12.285 mm	0.441 mm
05.03.23 – 12:30 (72 hours)	12.370 mm	0.085 mm
09.03.23 – 12:30 (168 hours)	12.436 mm	0.066 mm
Total		0.592 mm

Table 7: Result Halliburton blend specimen 2

Total expansion for specimen 2, in percent;

$$\boldsymbol{l}_{\Delta,\boldsymbol{SI}} = (\boldsymbol{l}_{\boldsymbol{f},\boldsymbol{SI}} - \boldsymbol{l}_{\boldsymbol{i},\boldsymbol{SI}})\ x\ 0{,}358 = (12{,}436\ mm - 11{,}844\ mm)\ x\ 0{,}358 = 0{,}212\ \%\ change$$

Specimen 3:

Time	Measured distance	Expansion
09.03.23 – 12:30	11.901 mm	0 mm
10.03.23 – 12:30 (24 hours)	12.324 mm	0.423 mm
12.03.23 – 12:30 (72 hours)	12.450 mm	0.126 mm
16.03.23 – 12:30 (168 hours)	12.515 mm	0.065 mm
Total		0.614 mm

Table 8: Result Halliburton blend specimen 3

Total expansion for specimen 3, in percent;

$$\boldsymbol{l}_{\Delta,\boldsymbol{SI}} = (\boldsymbol{l}_{\boldsymbol{f},\boldsymbol{SI}} - \boldsymbol{l}_{\boldsymbol{i},\boldsymbol{SI}})\ x\ 0{,}358 = (12{,}515\ mm - 11{,}901\ mm)\ x\ 0{,}358 = 0{,}220\ \%\ change$$

Halliburton blend graphs:

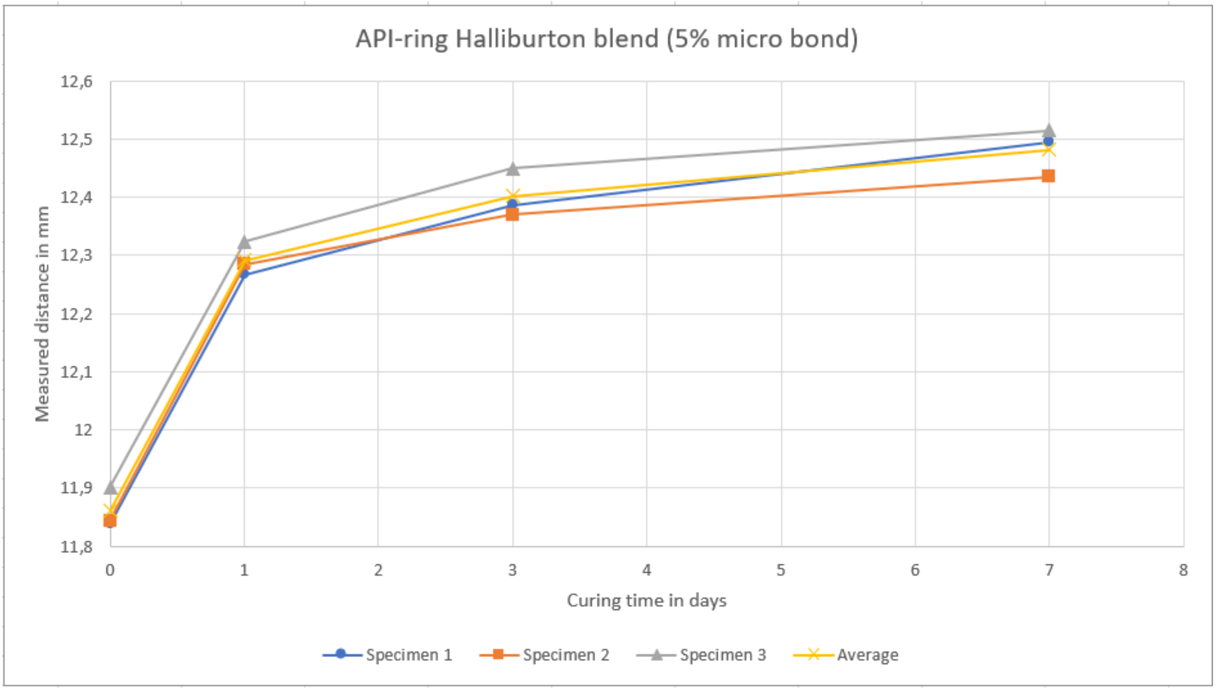

Figure 11: API-ring Halliburton blend graphs

4.5 Discussion API ring

Average Neat Class-G

Time	Measured distance	Expansion
0	11.878 mm	0 mm
24 hours	12.328 mm	0.450 mm
72 hours	12.342 mm	0.014 mm
168 hours	12.354 mm	0.012 mm
Total		0.476 mm

Table 9: API-ring average Neat Class-G

We can clearly see that most of the expansion for the Class-G happens within the first 24 hours.

$$\text{Percent of total expansion within first 24 hours: } \frac{Expansion\ after\ 24\ hours}{Total\ expansion} \times 100\%$$

$$\text{Percent of total expansion within first 24 hours: } \frac{12{,}328\ mm}{12{,}354\ mm} \times 100\% = 94{,}54\%$$

Average Halliburton blend (5% MicroBond)

Time	Measured distance	Expansion
0	11.861 mm	0 mm
24 hours	12.292 mm	0.431 mm
72 hours	12.402 mm	0.110 mm
168 hours	12.482 mm	0.080 mm
Total		0.621 mm

Table 10: API-ring average Halliburton blend

The Halliburton blend also makes a big part of its expansion during the first 24 hours but not as much as the Class-G. This slurry keeps on expanding during the entire curing time.

$$\text{Percent of total expansion within first 24 hours: } \frac{Expansion\ after\ 24\ hours}{Total\ expansion} \times 100\%$$

$$\text{Percent of total expansion within first 24 hours: } \frac{12{,}292\ mm}{12{,}482\ mm} \times 100\% = 69{,}40\%$$

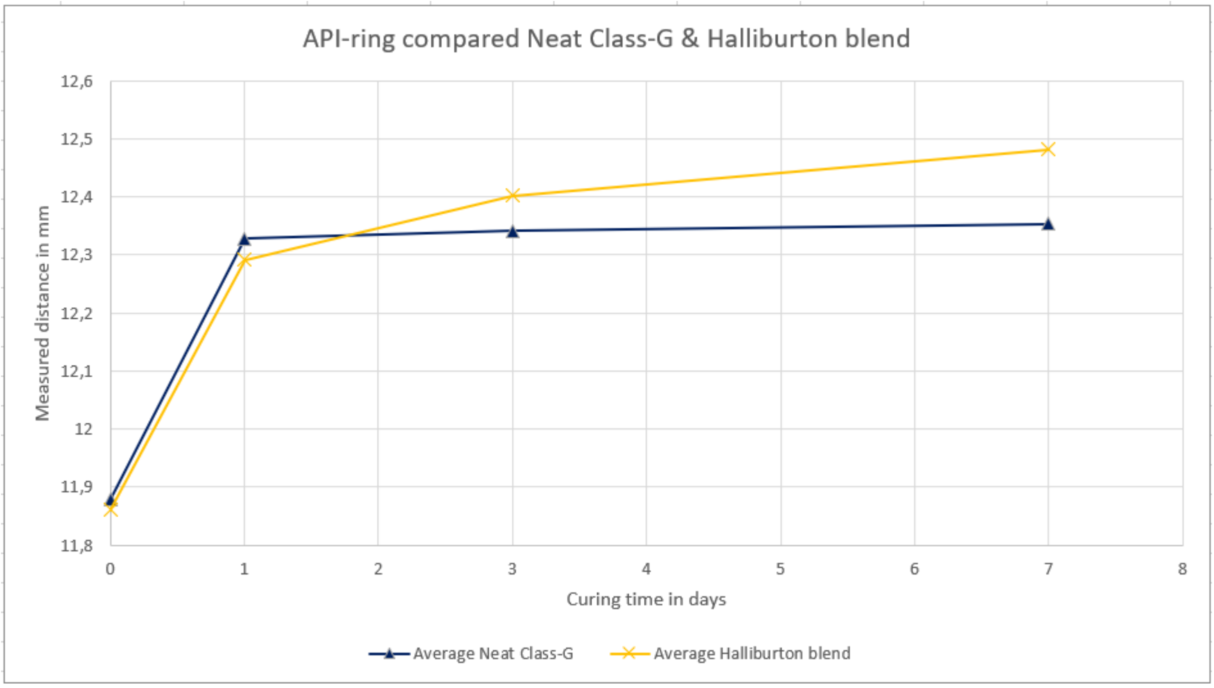

Figure 12: API-ring compared graphs

When looking at these graphs we can notice some interesting differences with the two slurries. We can see that they behave quite similarly after 24 hours, but from there they have different behaviour. The Class-G seems to have reached close to its maximum expansion, unlike the Halliburton blend which keeps expanding during the entire curing time. Even though most of its expansion happens within the first 24 hours.

These are valuable factors for us to know when we proceed with further push-out testing. One of the reasons we do this test is to learn more about how the different slurries behave to better understand and make conclusions in our main test, the repeated push-out test. From our calculations we know that 94% of Class-G expansion happens within the first 24 hours compared to the Halliburton blend which has 69% of its expansion within the same timeframe.

Total average expansion for Neat Class-G, in percent;
$l_{avg,Neat}$ = 0,170%

Total average expansion for Halliburton blend, in percent;
$l_{avg,Halliburton}$ = 0,222%

Difference

$l_{avg,Halliburton} - l_{avg,Neat}$ = 0,222% - 0,170% = 0,052%

Although the expansion rate may appear insignificant, it is important to avoid excessive expansion, as it can give rise to various complications such as fracturing formation.

If cement slurries expand excessively in oil wells, it can cause several issues. For instant it can reduce mechanical strength because excessive expansion can lead to a reduction in the mechanical strength of the cement sheath, making it more prone to cracking or failure under stress. Another complication can be loss of zonal isolation. When the cement slurry expands beyond the expected range, it can cause annular pressure build-up, leading to the loss of zonal isolation between different formations. Over-expansion can also cause cement to channel, leading to incomplete zonal isolation, which can result in fluid migration or loss of well integrity. Excessive cement expansion can also reduce the wellbore diameter, causing difficulties in running completion equipment or even blocking the wellbore completely.

Therefore, it is crucial to maintain the expansion of cement slurries within the recommended range to ensure effective zonal isolation and maintain well integrity. The recommended linear expansion for cement slurries in oil wells depends on various factors such as well conditions, temperature, pressure, and type of cement used. Based on our results we can say that linear expansion for our slurries varies around 0.1% to 0.3%. It is essential to carefully design and test the cement slurry to ensure that the linear expansion falls within the desired range to maintain well integrity and prevent any complications.

5. Volumetric expansion test

This experiment can help us understand the behaviour of concrete under different conditions, such as changes in temperature, humidity, and loading. Volumetric change experiments can also provide insights into the durability of concrete and its resistance to cracking, shrinkage, expansion, and deformation over time. This information is crucial for the design of cementing operations. In addition to this, we also wanted to investigate the correlation between linear expansion and volumetric expansion based on mathematical expressions.

From the API-ring Table 9 and 10, we knew that the Neat Class-G cement had almost 95% of its expansion happen within the first 24 hours. Therefore, we opted to do the volumetric expansion test only on the Halliburton blend as it would bring the most interesting results with noticeable expansion over the entire test period.

5.1 Engineering/designing setup

This test is not from an API or ISO standard and must be seen as experimental testing. We developed the test in collaboration with our supervisor and his PhD student. We have used the API recommended practice 10B-5, also known as ISO 10426-5, as a guideline. Chapter 6 in API 10B-5 told us about determination of bulk shrinkage or expansion under impermeable condition and atmospheric pressure, using a membrane test. We did not have access to such equipment, so we decided to do an approach without electronic measurements.

We started from the fact that if you put something inside water in a container and that thing expands, the water level will rise. So, with this in mind, we started thinking of possible solutions. We knew we needed to have a big enough container to fit a setup with approximately 600 ml of slurry. There were ordered special medical balloons specifically for this test-setup.

Figure 13: Volumetric setup and balloon

To make the setup useable, we drilled a hole in the container and attached a hose to it, so the water can overflow as the slurry expands in the balloon. We used silicon to attach the hose to the container. The silicon we used was water resistant, making the area around the hose completely sealed. This was constructed and left for 24 hours before we tested it to check that it did not leak. The hose was connected down into a measurement cylinder, which we weighed to get the exact amount of water that came out.

We had to do three different setups to optimize the testing, because we met difficulties or saw improvements that could be done. The first attempt we started by taking a big container which fit around 12 litres. This one gave us difficulties because if the big quantity of water was exposed to movement, it easier overflowed and gave us incorrect results. For the second setup we used a smaller container and did the setup in the exact same way. The problem with this was that there was no water overflowing. We suspected that this was due to the angle on the hose and the fact that there could be a vacuum inside the hose. For the final setup we used the same container but replaced the hose with one with a bigger diameter. By doing this the water had a freer way of flowing, giving us more accurate results. In addition, we used a tape to get a steeper angle on the hose down into the measuring cylinder. We also had a lid placed on top of the container that prevented the water from evaporating and sealed the system.

Developed setups:

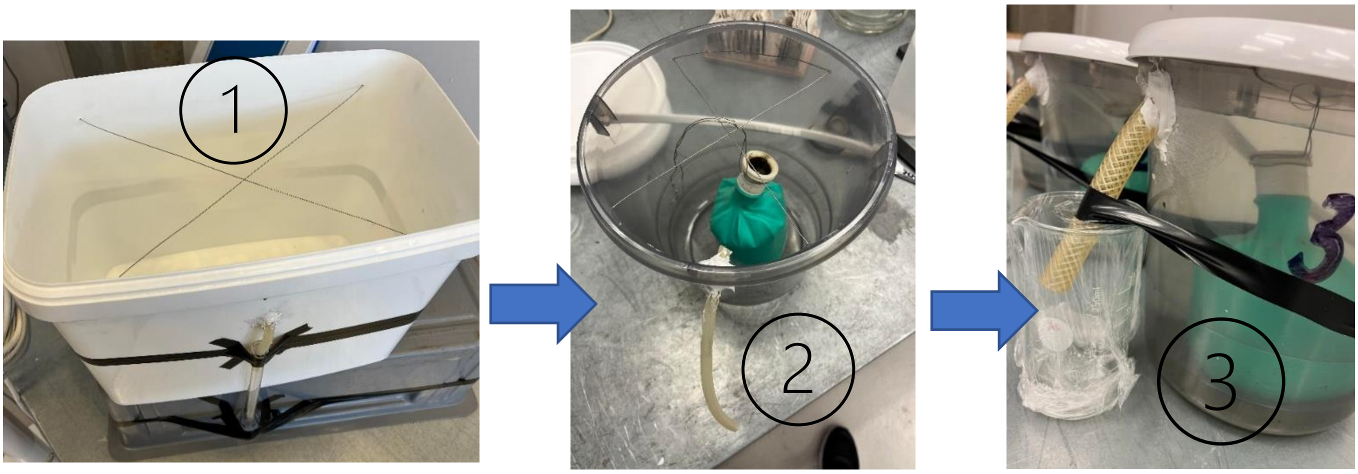

Figure 14: Engineering of volumetric setup

By doing it this way, we came up with an optimized setup that worked according to our preferences. After completing this engineering phase and deciding on the main design, we made two more identical setups. This made it possible for us to run three identical tests at the same time and giving us a better baseline to analyze the results using three independent tests.

We decided to bring this design and engineering process into the thesis to show some of the process we went through and some of the work that is behind a setup like this.

5.2 Procedure

Step 1:

Initially, we proceeded by filling three containers with water. To be able to have control on the amount of water, we weighted the full bucket and subtracted the weight of the empty bucket. We ensured that sufficient water was added to the containers, such as they reached their full capacity and began overflowing. Subsequently, we measured the weight of the overflowed water to determine the exact quantity of water inside the containers.

Step 2:

Prepared and made the slurry according to 3.2, 3.3 and Table 2. We used the same recipe as in the API ring testing, making three independent specimens. As previously mentioned, we opted to use Halliburton blend for this experiment.

Step 3:

Following the preparation of the slurry, it is necessary to dispense it into the balloons using a funnel. An effort is made to transfer the maximum quantity of slurry from the mixing cup into the balloon. Upon completion of filling, the weight of the balloon is recorded. Before this, a measurement is taken to determine the weight of the empty balloon. By subtracting the weight of the balloon from the total weight, the weight of the slurry contained within the balloon can be found. This information is significant in the ensuing calculations and result analysis.

Step 4:

The installation of the balloon within the container is achieved by fastening it to custom-made steel wires, which serve to maintain the balloon's form and prevent spillage of the slurry. Upon balloon installation, some water will once again overflow and be accumulated within a measurement cylinder. The weight of this water is also measured and subtracted from the initial amount of water added, resulting in a new measurement of the net zero amount of water. We also make sure that the water has completely stopped overflowing.

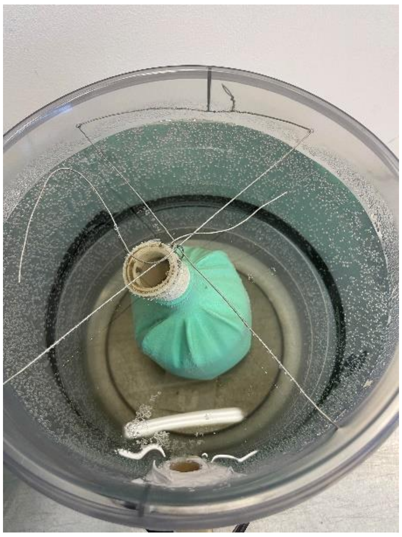

Figure 15: Volumetric balloon setup

Step 5:

The last step is to make sure that the measurement cylinder is empty and located under the hose. We put some clingwrap in between the open space between the hose and the cylinder. This makes the setup almost airtight and prevents the water coming out of the container from evaporating. We check the tests after 24 hours, 72 hours and at last after the seven days has been completed. To know how much water that has been released out due to the expansion we weigh the measurement cylinder and subtract the weight of the cylinder itself.

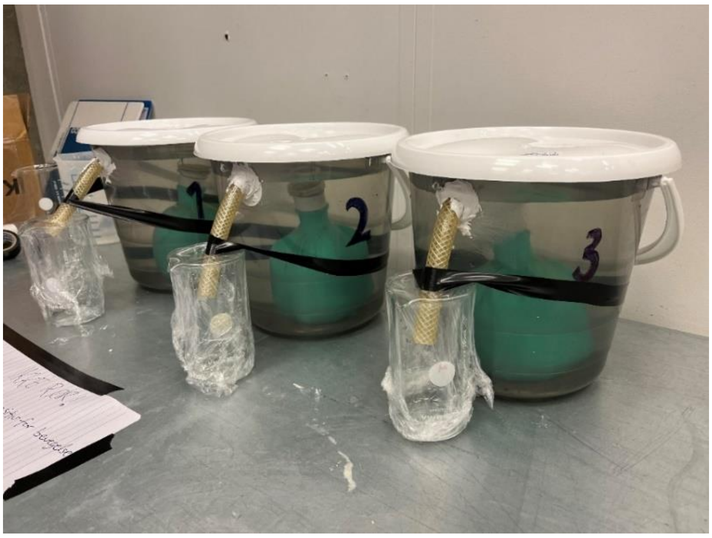

Figure 16: Volumetric expansion experiment

5.3 Results volumetric expansion

Days	TEST 1	TEST 2	TEST 3
0	118,12 g	116,04 g	118,18 g
1	118,20 g	116,15 g	118,30 g
3	119,73 g	117,56 g	120,05 g
7	121,81 g	119,63 g	122,70 g
TOTAL	3,69 g = 3,69 ml	3,59 g = 3,59 ml	4,52 g = 4,52 ml

Table 11: Volumetric expansion results

Table 11 shows the weight of the overflowed water and measurement cylinder. Which means that the day 0 value is just the weight of the empty cylinder + the clingwrap. From these values we find the volumetric expansion in ml.

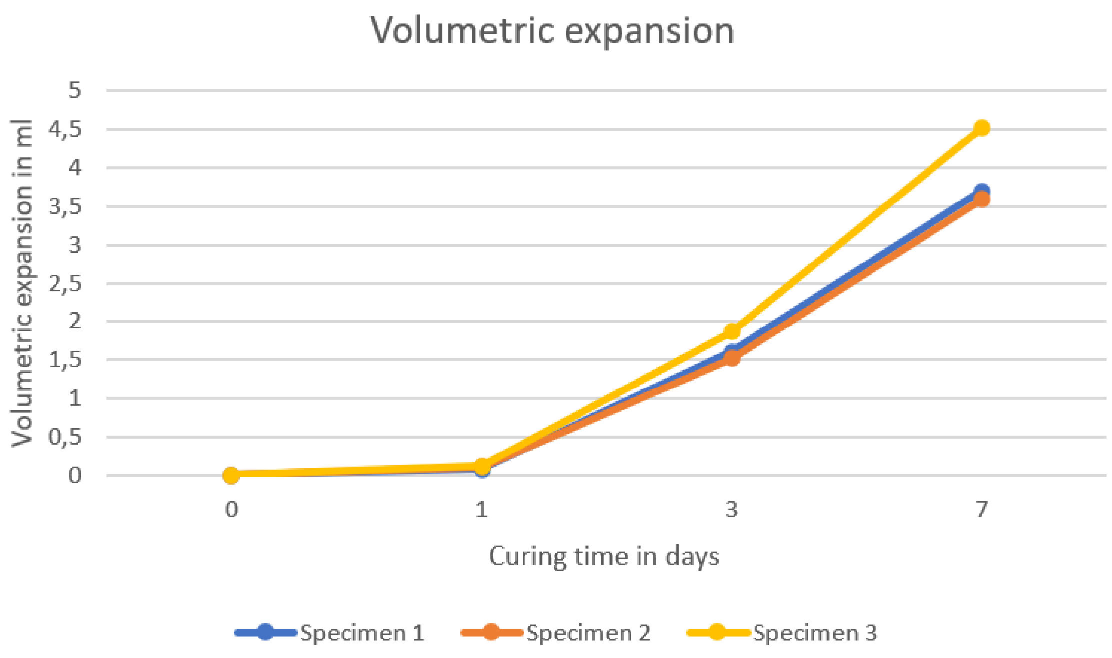

Figure 17: Volumetric expansion graph

The slurry has a density of 1,91 kg/l according to the data sheet.

Test 1:

Weight of cement slurry = measured weight – balloon weight = 1002,0 g – 18 g = 984,0 g

Volume of cement = $\frac{\text{Mass}}{\text{Density}} = \frac{0{,}984\ \text{kg}}{1{,}91\ \text{kg}/_\text{l}}$ = 0,51518 l = 515,18 ml

Volumetric change, in percent = $\frac{\text{Volume change}}{\text{Total volume}} = \frac{3{,}69\ \text{ml}}{515{,}18\ \text{ml}}$ × 100 % = 0,716 %

Test 2:

Weight of cement slurry = 1003,2 g – 18 g = 985,3 g

Volume of cement = $\frac{0{,}9852\ \text{kg}}{1{,}91\ \text{kg}/_\text{l}}$ = 0,51581 l = 515,81 ml

Volumetric change, in percent = $\frac{3{,}59\ \text{ml}}{515{,}81\ \text{ml}}$ × 100 % = 0,696 %

Test 3:

Weight of cement slurry = 1008,3 g – 18 g = 990,3 g

Volume of cement = $\frac{0{,}9903\ \text{kg}}{1{,}91\ \text{kg}/_\text{l}}$ = 0,51848 l = 518,48 ml

Volumetric change, in percent = $\frac{4{,}52\ \text{ml}}{518{,}48\ \text{ml}}$ × 100 % = 0,872 %

5.4 Formula and calculations

Expansion of a cement plug:

To be able to make connection between the linear expansion and the volumetric expansion there has been derived an equation describing this relation.

Equation 4) Before expansion: $\boldsymbol{V_0} = \pi r^2 L$

Equation 4: Before expansion, V0

Equation 5) After expansion: $\boldsymbol{V_1} = \pi(r + \Delta r)^2(L + \Delta L)$

Equation 5: After expansion, V1

Equation 6) Linear expansion coefficient: $\boldsymbol{\beta} = \frac{\Delta r}{r} = \frac{\Delta L}{L}$

Equation 6: Linear expansion coefficient, Betta

Equation 7) Expansion volume: $\frac{\boldsymbol{\Delta V}}{\boldsymbol{V_0}} = (1+\beta)^3 - 1$

Equation 7: Expansion volume

Equation 8) Combined all equations above: $\frac{\boldsymbol{\Delta V}}{\boldsymbol{V_0}} = (1+\beta)^3 - 1$

Equation 8: Combined eq.4-7

Equation 9) Rearranged equation 8: $\boldsymbol{\beta} = \sqrt[3]{1 + \Delta V/V_0} - 1$

Equation 9: Rearranged eq.8

If the results should be able to represent this relation, we wish to keep:

0.1% ≤ $\boldsymbol{\beta}$ ≤ 0.4%, which gives us that 0.3% ≤ $\boldsymbol{\Delta V/V_0}$ ≤ 1.2%

By using equation 9 we can calculate the β factor for our results:

$$\beta_1 = \sqrt[3]{1 + \frac{\Delta V}{V_0}} - 1 = \sqrt[3]{1 + \frac{3{,}69}{515{,}18}} - 1 = 0{,}0023818$$

$\underline{\underline{\beta_1 = 1 * \beta_1 = 100\% * 0{,}0023818 = 0{,}238\%}}$

$$\beta_2 = \sqrt[3]{1 + \frac{\Delta V}{V_0}} - 1 = \sqrt[3]{1 + \frac{3{,}59}{515{,}81}} - 1 = 0{,}0023146$$

$\underline{\underline{\beta_2 = 1 * \beta_2 = 100\% * 0{,}0023146 = 0{,}231\%}}$

$$\beta_3 = \sqrt[3]{1 + \frac{\Delta V}{V_0}} - 1 = \sqrt[3]{1 + \frac{4{,}52}{518{,}48}} - 1 = 0{,}0028975$$

$\underline{\underline{\beta_3 = 1 * \beta_3 = 100\% * 0{,}0028975 = 0{,}290\%}}$

5.5 Discussion volumetric expansion

Average percent calculated from β in volumetric experiment:

$$\beta_{avg} = \frac{0{,}238\% + 0{,}231\% + \ 0{,}290\%}{3} = 0{,}253\%$$

Average linear change from API ring, in percent:

$$API\ Ring_{avg} = \frac{0{,}235\% + 0{,}212\% + \ 0{,}220\%}{3} = 0{,}222\%$$

Accuracy in percent:

$$\frac{\beta_{avg}}{API\ Ring_{avg}} = \frac{0{,}253\%}{0{,}222\%} = 0{,}8787 = 87{,}9\ \%$$

Based on the present calculation, it is clear that this methodology provides a reliable means of determining the mathematical correlation between linear expansion and volumetric expansion. This opens a broader spectrum of potential applications for conducting such experiments. For instance, one can invert the formula and approximate the volumetric change from the outcome obtained in a linear expansion test, such as the API ring test.

6. Repeated push-out testing in 100 kN MTS machine

We wanted to use repeated push-out testing to investigate the effect time and repeated pushing had on the bond strength for shear resistance between interfaces. In addition, this study also examined the failure process of bond surfaces under shear action and the strain development on the cement plug.

6.1 Casing pipe size and roughness

We started by taking diameter measurements of the pipes we were using in the experiment. These values were used for calculations later. The roughness of the pipes was also measured. We did not use the roughness for calculation, but we wanted to measure it to have more of an understanding of how rough the pipes are and as an indication of the friction between pipe and cement. Ra and Rz are parameters used to measure surface roughness, where Ra represents the average roughness of a surface, while Rz refers to the vertical distance between the highest peak and the lowest valley in the surface.

Casing number	Roughness	Inner diameter
1	Ra = 0.751 µm Rz = 3.843 µm	ϕ = 112.10 mm
2	Ra = 0.730 µm Rz = 3.938 µm	ϕ = 112.12 mm
3	Ra = 0.807 µm Rz= 4.139 µm	ϕ = 112.05 mm

Table 12: Casing roughness and diameter

6.2 Procedure

Step 1:

Our initial step involves affixing the three casing pipes to the lower plate by using adhesive material to ensure a fully enclosed configuration that prevents any leakage of the cement slurry. Additionally, we cover the bottom plate with clingwrap to prevent the cement from adhering and enable effortless removal of the bottom plate. The bottom plate and the casing pipes are then sealed with water resistant silicon, and we let this sit to harden for 24 hours.

Figure 18: Casing and bottom plate

Step 2:

After the silicon has hardened, we are ready for the next step: mixing the slurry and filling the casing with approximately 600 ml slurry. Again, we used the same recipes as in the previous testing, for batch 1 we used the Neat Class-G recipe and for batch 2 we used the Halliburton blend. For more detailed information about the recipes and mixing, look at 3.2, 3.3, Table 1 and Table 2.

Just like in the API ring testing, we made three independent specimens. We started making the Neat Class-G specimens and after completing all of the testing for these, we made the exact same setup for the Halliburton blend. We used the same casing and bottom plates for both batches to avoid making errors.

Step 3:

The casings are to be filled with the slurry and then placed in a container. The container is then carefully filled with water before placing a lid on top to make it airtight. We try to have it as similar as the API ring testing to achieve a better basis for connecting the results. Unlike the ring testing, we did not have the opportunity to cure the specimen in heated water (25°C), but they were stored under water at room temperature and atmospheric pressure.

Step 4:

The specimens were left to cure inside containers for 7 days before performing the first push-out tests. We then placed the specimens back into the same water and containers and left them to cure another 7 days, now for a total of 14 days. After completing the second push-out test, they were left to cure another 7 days, making it a total of 21 days. After completing the entire curing time, we ran the third and final push-out tests.

Figure 19: Casing in curing bath

6.3 Push-out testing

Step 1:

We start by preparing our samples, for the first test after 7 days we need to remove the bottom plate. This can easily be done by cutting the silicon with a knife and gently hitting the plate with at plastic hammer. After doing this, we ensure the sample is free from any additional cement around the casing wall. This is important because this access cement can damage the piston we are using for the push-out test. For our tests there was only one sample where we needed to remove some cement along the wall. This happened because there was a minor space between the bottom plate and the casing wall. For the testing after 14 and 21 days we can skip this part because the access cement is already removed.

Step 2:

After preparing the samples, the assembly process begins, which is relatively straightforward in this case. A 100 kN MTS machine is employed, which is connected to a computer preconfigured for data processing. Prior to initiating the sample testing, it is necessary to ensure that the piston is appropriately assembled and has a small clearance between the walls. Inadequate clearance may result in the piston becoming lodged in the casing wall, leading to damage and undesirable outcomes. The objective of this test is to evaluate the strength the shear bond between the cement and the casing; hence, the piston must not exert pressure on the walls.

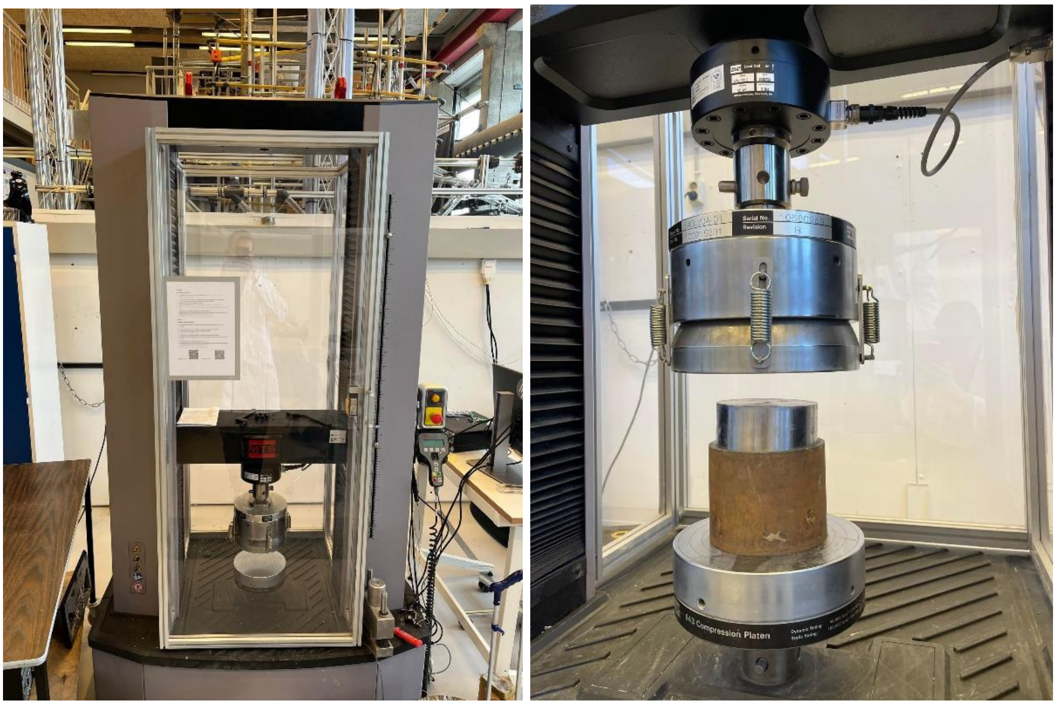

Figure 20: MTS machine and piston

Step 3:

Once the setup has been prepared, testing commences. The first step involves inserting the filled casing and piston into the machine, as illustrated in Figure 20. The pushing head of the machine is then adjusted manually, to position it as close to the piston as possible without making contact. The pushing head is equipped with springs that enable load adjustment and distribution across the entire piston surface, even if it is not entirely level. Thereafter, the push-out procedure is initiated using a preconfigured computer template that incorporates the relevant values. The machine is designed to apply force slowly until it reaches 0.100 kN to ensure complete and even load distribution across the piston.

Figure 21: Push-out testing

Subsequently, the machine applies pressure until the cement begins to move, which produces a peak that indicates the maximum load the cement can withstand. This measure is related to the shear bond between the cement and the casing, and the point at which movement begins is referred to as bond-slip, which will be discussed later in this thesis. Testing is conducted over a 30 mm interval, with the machine set to displace the plug at a rate of 1 mm/min.

Step 4:

The sample is flipped 180 degrees following the initial front-push, and the same test is repeated. This is referred to as the back-push or second push and provides insight into the resistance following the destruction of the initial shear bond. Further details regarding this aspect will be presented in the results and conclusion sections.

Step 5:

After completing the front and back-push, the samples are returned to their curing baths and left for an additional 7 days, bringing the total curing time to 14 days, before repeating the same testing procedure. After the second round of testing, the samples are once again left to cure for 7 days, bringing the total curing time to 21 days, before conducting the final push-out tests. This methodology enables us to obtain crucial information on how time and mechanical activity impacts the bonding between the cement and the casing.

6.4 Results push-out testing

We observed during all push-out tests that our graphs are quite “noisy”. There is a lot of fluctuations up and down in the load values. The machine is set to take around twenty measurements each second making a lot of measurement points. One of the reasons for these variations in the values, is stick-slip effect. The stick-slip effect, also known as stiction, is a phenomenon that occurs when two surfaces in contact intermittently stick and then slip relative to one another.

The cement plug is being pushed down until it sticks to the pipe and the load increases before the plug slips again, and the load required to move it is decreased. When a force is applied to a system experiencing the stick-slip effect, the surfaces initially stick together, resisting the applied force. As the force continues to increase, the surfaces eventually reach a threshold where they suddenly slip and move relative to one another. This effect happens repeatedly so the push-load is continuously increasing and decreasing. We want to show this effect and have therefore made plots for all the results with every measurement from the machine setup.

The roughness measurements, particularly the Rz parameter which quantifies the difference between the highest peak and lowest value, reveal differences in the roughness of the surfaces that can significantly affect the stick-slip effect.

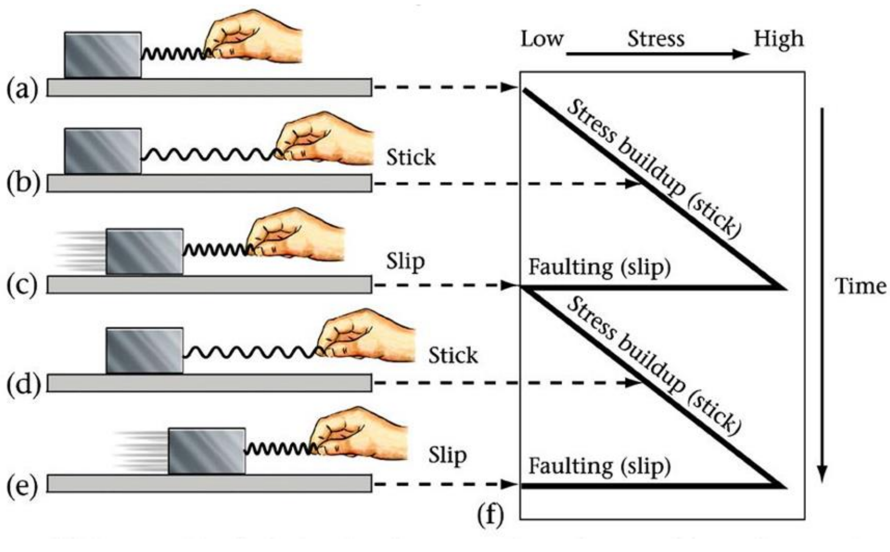

Figure 22: Stick-slip effect

6.4.1 Batch 1, Neat Class-G: Specimen 1-3.

After 7 days curing time:

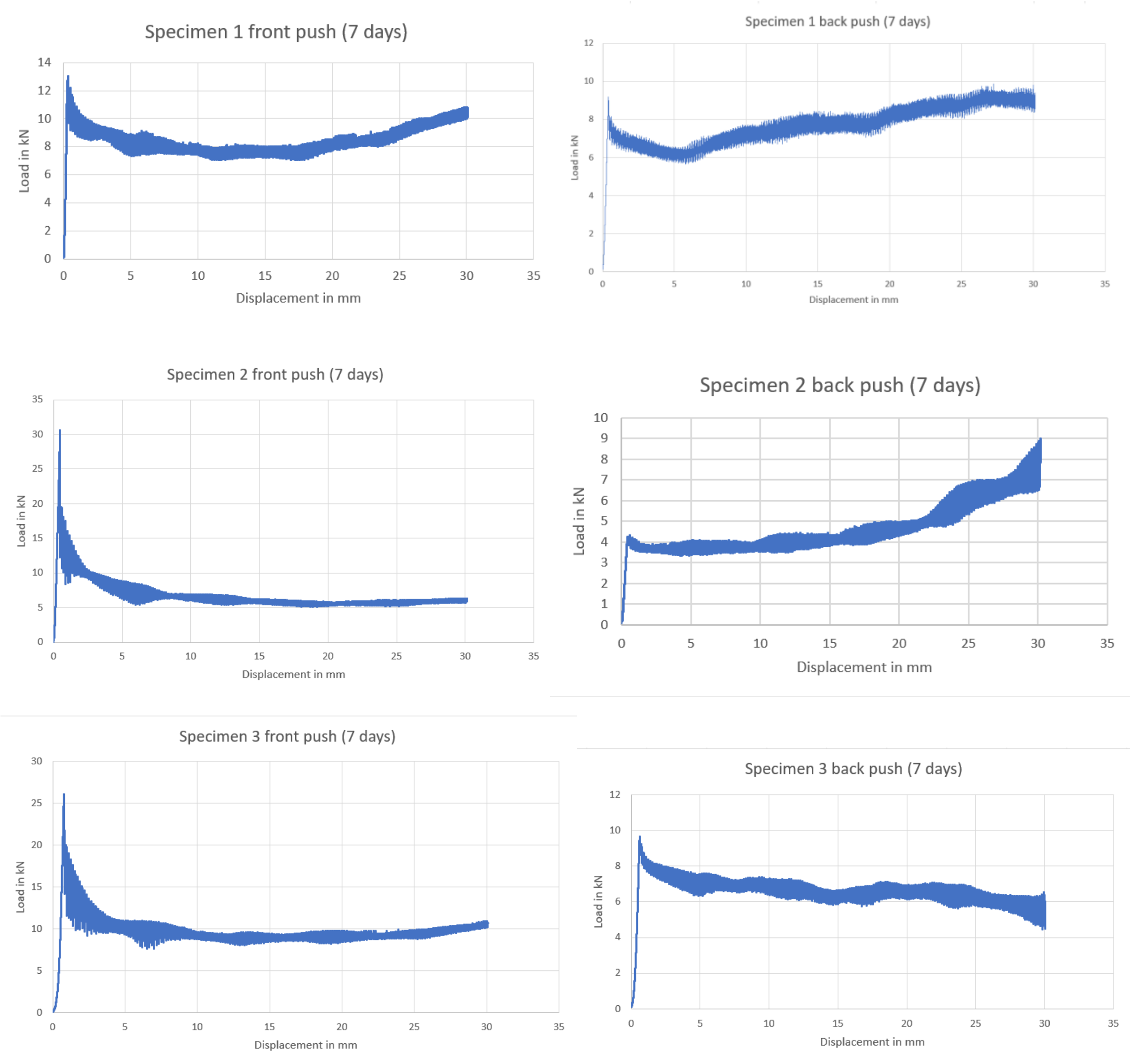

Figure 23: Push-out graph specimen 1-3, 7 days

Comments:

Specimen 1 exhibits a significantly lower peak value than specimens 2 and 3, measuring at almost half of their respective values. We hypothesize that this discrepancy may be attributed to a failure in bonding. However, the back-pushes remain consistent, and the values correspond well with the required load for pushing the cement plug. The behaviour in the back-push varies greatly due to how much resistance force is applied to the plug based on the different casings. We acknowledge the atypical peak value for specimen 1 and will monitor the subsequent results to observe its response.

After 14 days of curing time:

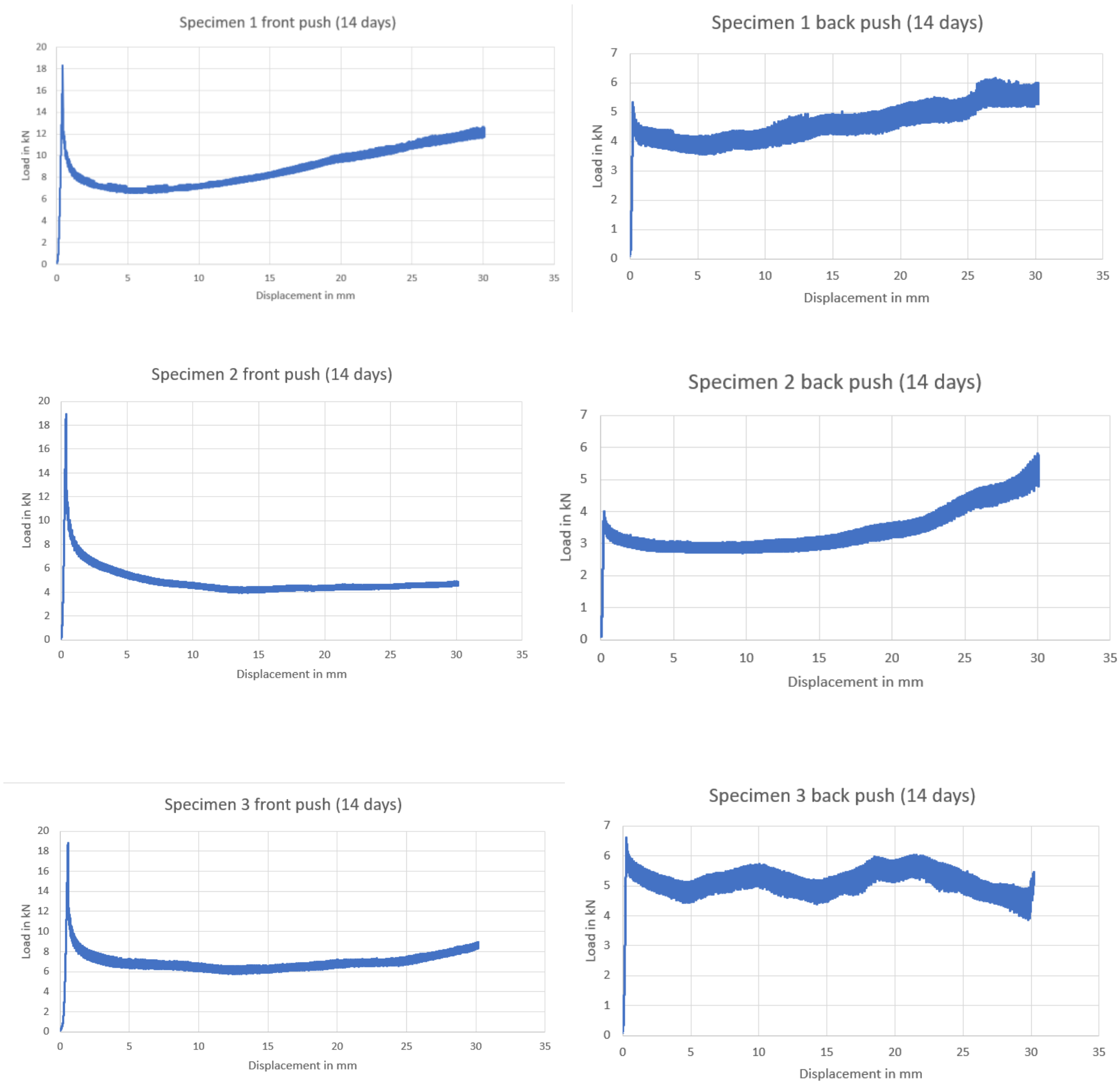

Figure 24: Push-out graph specimen 1-3, 14 days

Comments:

In the second push-out test round of batch 1, a distinct modification in the behaviour of specimen 1 is evident. All three peaks exhibit a nearly identical range of 18-19 kN. This value exceeds the peak magnitude observed during the first round of testing for specimen 1. This result suggests that the bonding procedure can generate a robust bond even after displacing the material.

After 21 days of curing time:

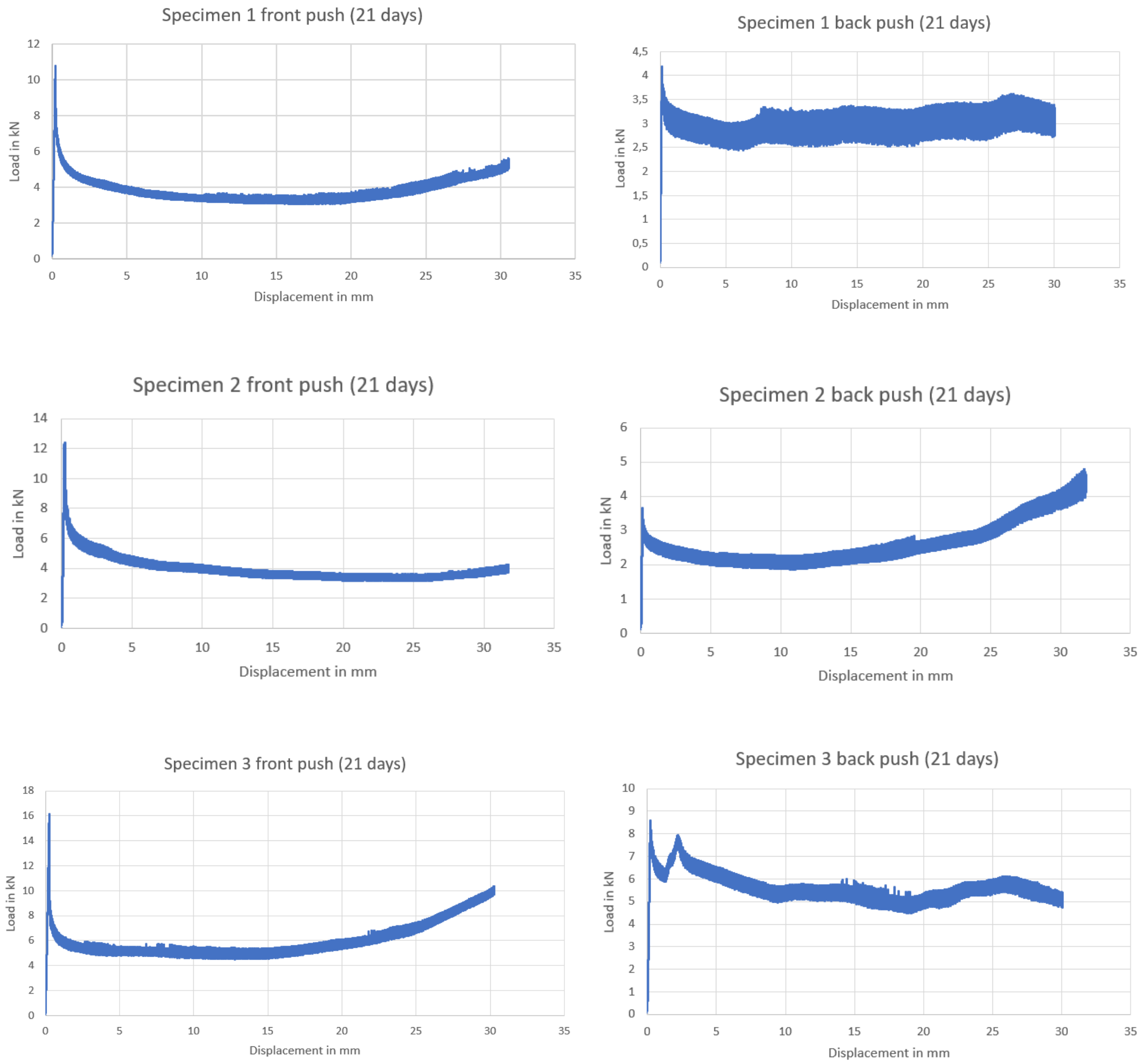

Figure 25: Push-out graph specimen 1-3, 21 days

Comments:

The peak loads observed during the push-out test after 21 days curing remain consistent within a range of 11-16 kN. Further data analysis reveals a noticeable, almost linear, decrease in peak loads over time, which will be discussed in detail later in the thesis.

6.4.2 Batch 2, Halliburton blend (5% MicroBond): Specimen 4-6

After 7 days of curing time:

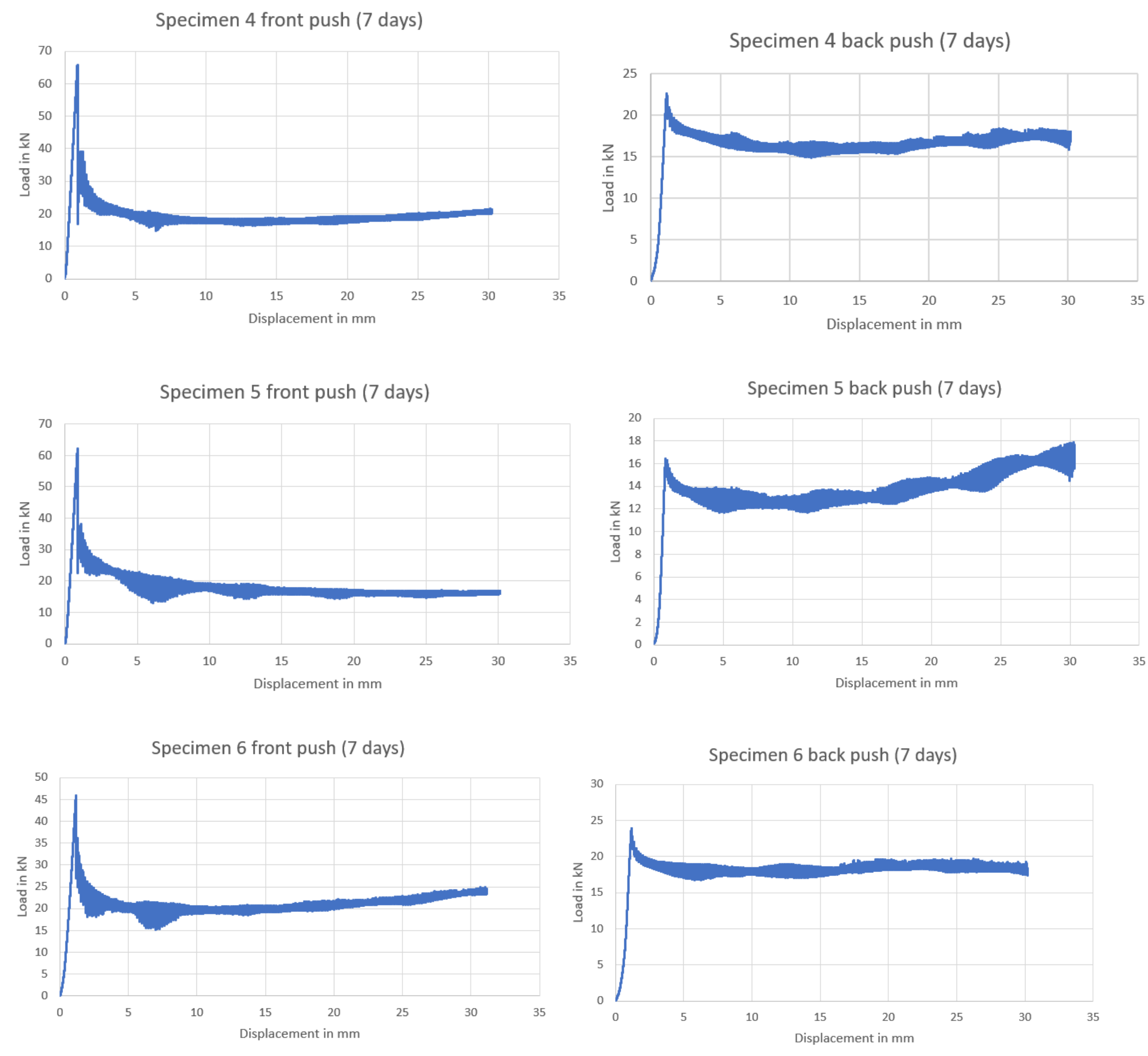

Figure 26: Push-out graph specimen 4-6, 7 days

Comments:

Through analysis of the push-out test results of batch 2, a notable difference in the peak loads was observed compared to those of batch 1. Additionally, specimen 6 presented substantially lower peak loads than specimens 4 and 5. Which we also saw a similar example of in batch 1. Further examination of these observations will be carried out to evaluate their developmental pattern. The back-push responses observed during the test corresponded to the essential force needed to displace the cement plug.

After 14 days of curing time:

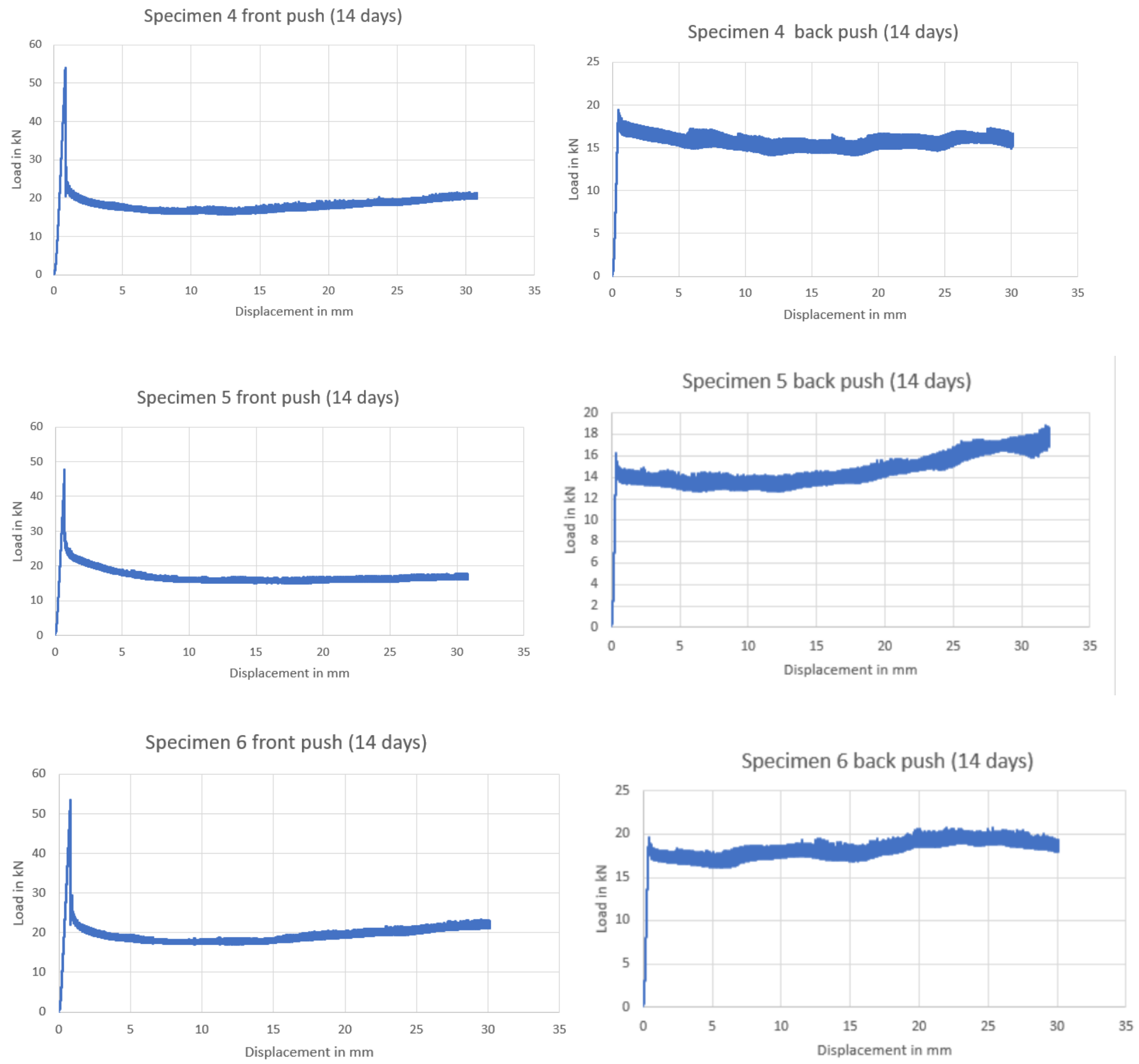

Figure 27: Push-out graph specimen 4-6, 14 days

Comments:

The push-out test results after 14 days demonstrate greater uniformity than those after 7 days, with peak loads ranging from 48-52 kN. As expected, the peak loads are lower after already being pushed out once after seven days. Specimen 6 has an even higher peak load than it had after 7 days. Which is similar to the behaviour we noticed for specimen 1 in batch one.

After 21 days of curing time:

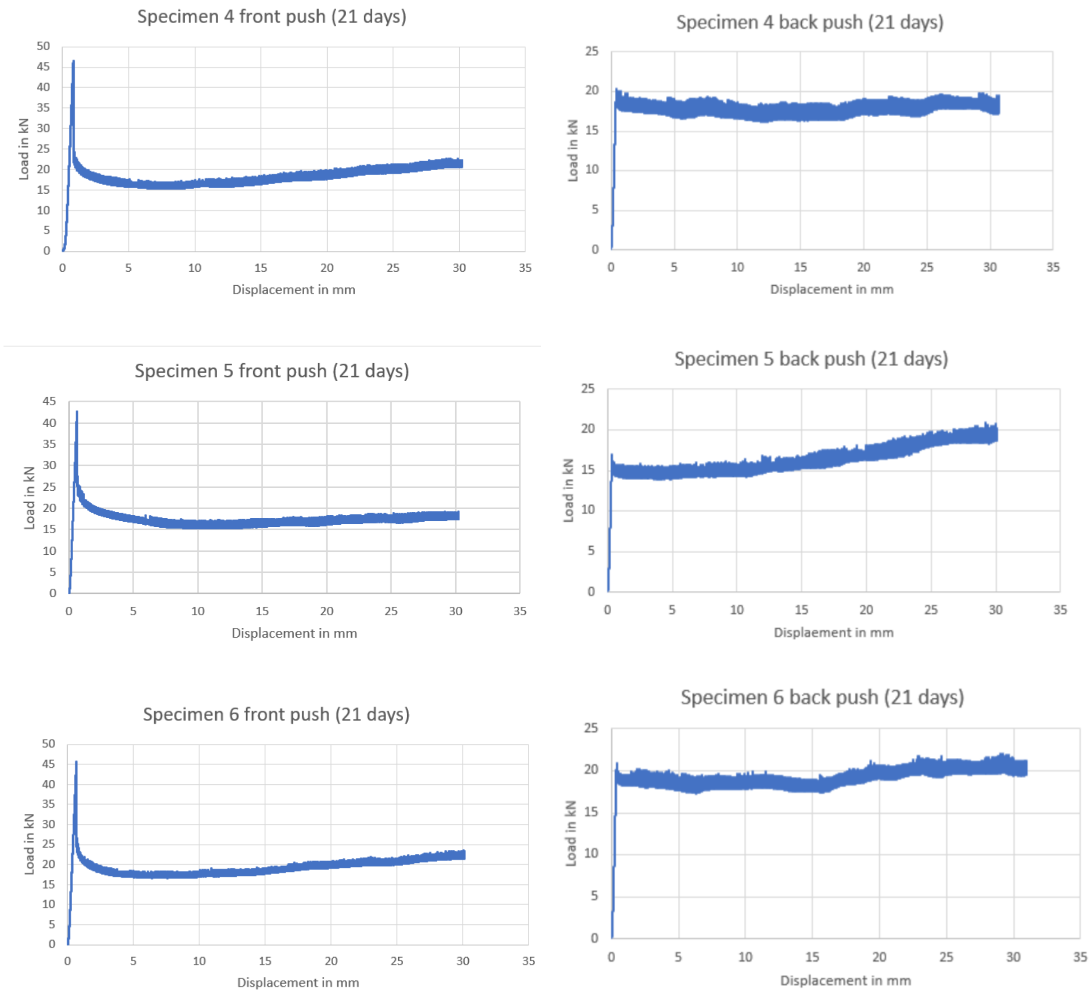

Figure 28: Push-out graph specimen 4-6, 21 days

Comments:

All three specimens behave very similarly, peaking at around 40-45 kN on the front-push and staying between 15-20 kN on the back-push.

6.5 Discussion push-out testing

To determine whether the expanding slurry exhibits stronger bonding properties than the Neat Class-G slurry, one of the most informative factors is the peak point, which represents the maximum force that the cement can withstand before it begins to move. Observing the peak point over a period of time is an important consideration. Furthermore, it is interesting that the plug can undergo re-bonding even after being subjected to multiple external forces. Although it is bonding again, it can't withstand the same load for the next pushes.

Average Peak load

Curing Days	Batch 1 Front-push	Batch 2 Front-push	Batch 1 Back-push	Batch 2 Back-push
7	23,23 kN	57,82 kN	9,52 kN	20,99 kN
14	18,7 kN	51,74 kN	5,59 kN	18,40 kN
21	13,11 kN	44,93 kN	5,48 kN	19,38 kN

Table 13: Average peak load

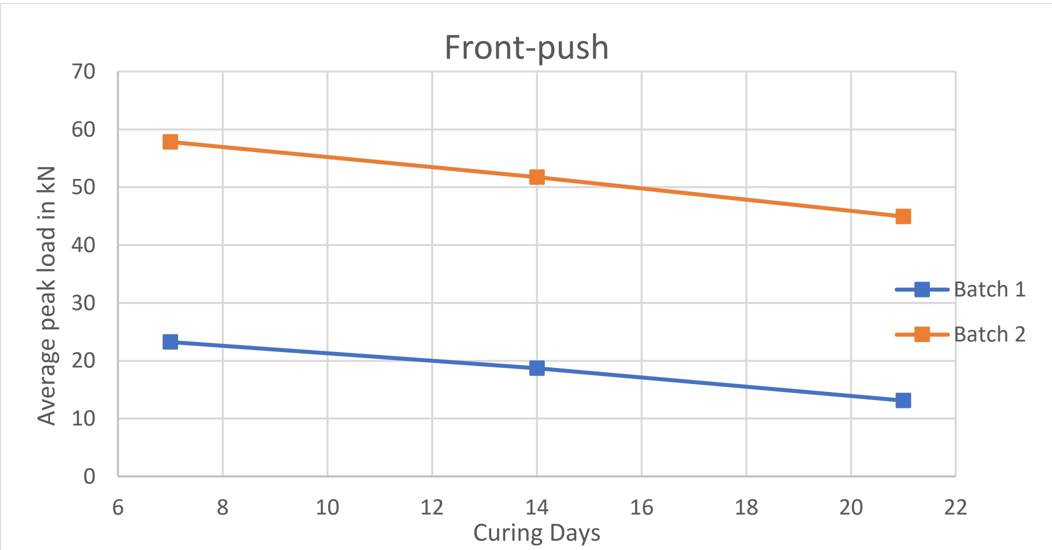

Figure 29: Average peak loads front-push

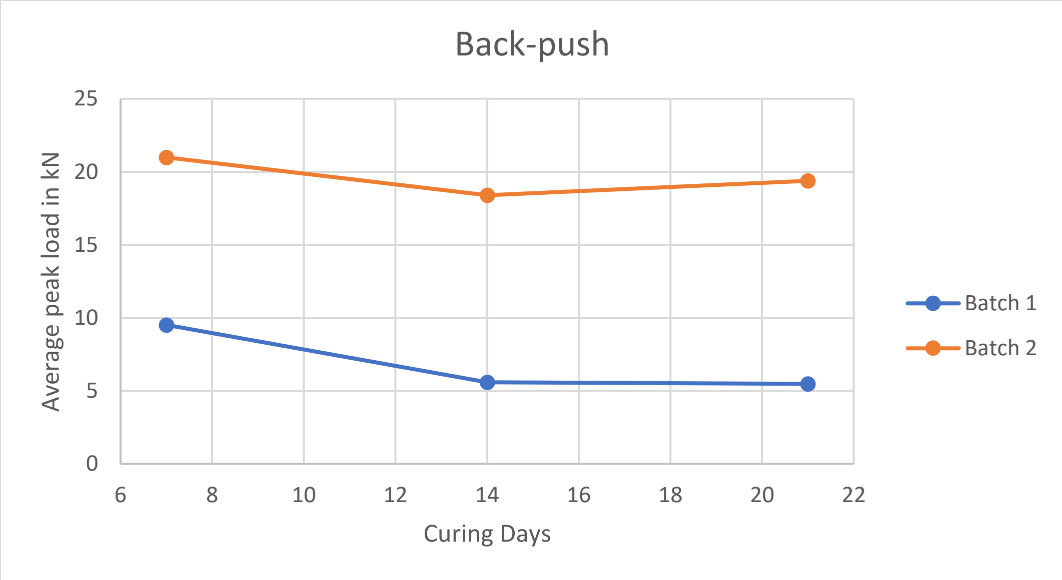

Figure 30: Average peak loads back-push

The visual representation in Figure 29 and 30 is based on average peak loads, and clearly show a notable difference in the amount of force needed to push the Neat Class-G plugs and the Halliburton blend plugs. Additionally, it is noteworthy that the evolution of peak load over time is almost linearly decreasing and relatively similar for both slurries. Therefore, based on the results, we can conclude that although the behaviours of the two slurries are nearly identical, the expansive slurry exhibits a higher load resistance capacity, indicating that the Halliburton blend possesses stronger properties.

We can also calculate the shear bond strength, giving us the same ratio but in pascal or bar. Shear bond strength, τ_{bs}, is determined by measuring the peak load, F_P, and dividing this force by the contact area between the cement and casing, A_c.

Shear bond strength: $\boldsymbol{\tau}_{\mathbf{bs}} = {A_c}/{\mathbf{F_p}}$

We want to determine the average shear bond strength of our tests, dividing them into four groups: Batch 1 front-push, Batch 1 back-push, Batch 2 front-push and finally Batch 2 back-push. All these groups have three different test runs, and we will calculate the average of all of them.

F_P = Average peak loads from Table 13

$A_c = 2\pi \cdot r \cdot h$ **h** = Average length of cement plugs = 58,123mm = 0,058123 m

d = from Table 12 **r** = $^{\mathbf{d}}/_{2}$= 56 mm = 0,056 m

$\mathbf{A_c}$ = 2π · 0,058123 · 0,056 = 0,02045 m^2

Using these values we calculated the average shear bond strength for each batch after the set curing days.

Example: Finding Average Shear bond strength for Batch 1 front push after 7 days

$$\tau_{bs} = \frac{23230\ N}{0{,}02045\ m^2} = 11357152{,}81\ \text{Pa} = 11{,}36\ \text{bar}$$

All the results are shown in Table 14.

Average Shear bond strength

Curing Days	Batch 1 Front-push	Batch 2 Front-push	Batch 1 Back-push	Batch 2 Back-push
7	11,36 bar	28,27 bar	4,65 bar	10,26 bar
14	9,14 bar	25,30 bar	2,73 bar	8,99 bar
21	6,41 bar	21,97 bar	2,68 bar	9,48 bar

Table 14: Average shear bond strength

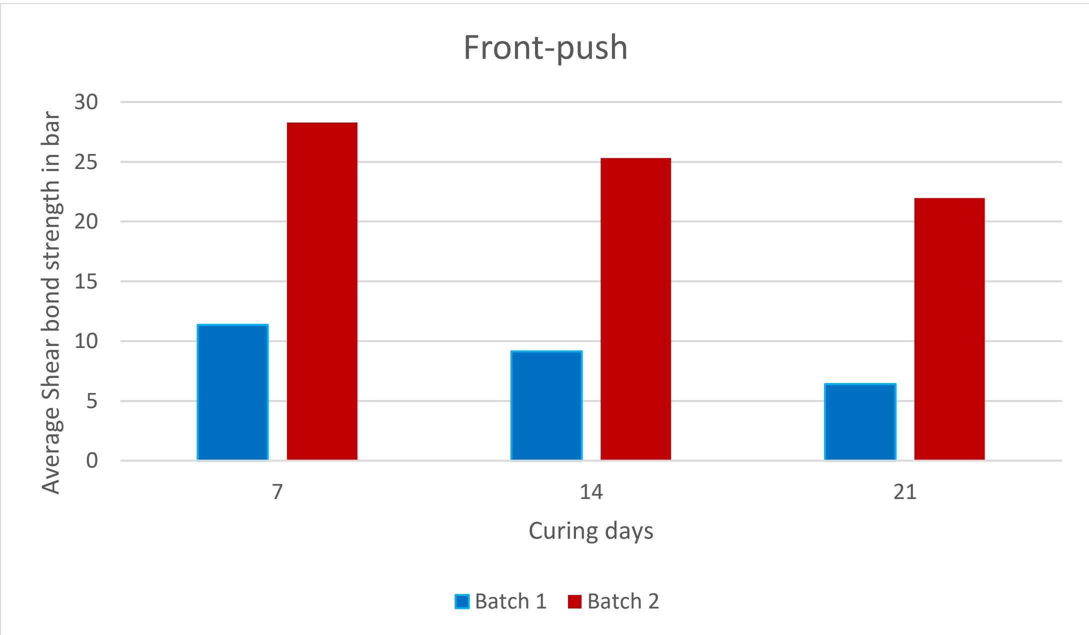

Figure 31: Average shear bond strength front-push

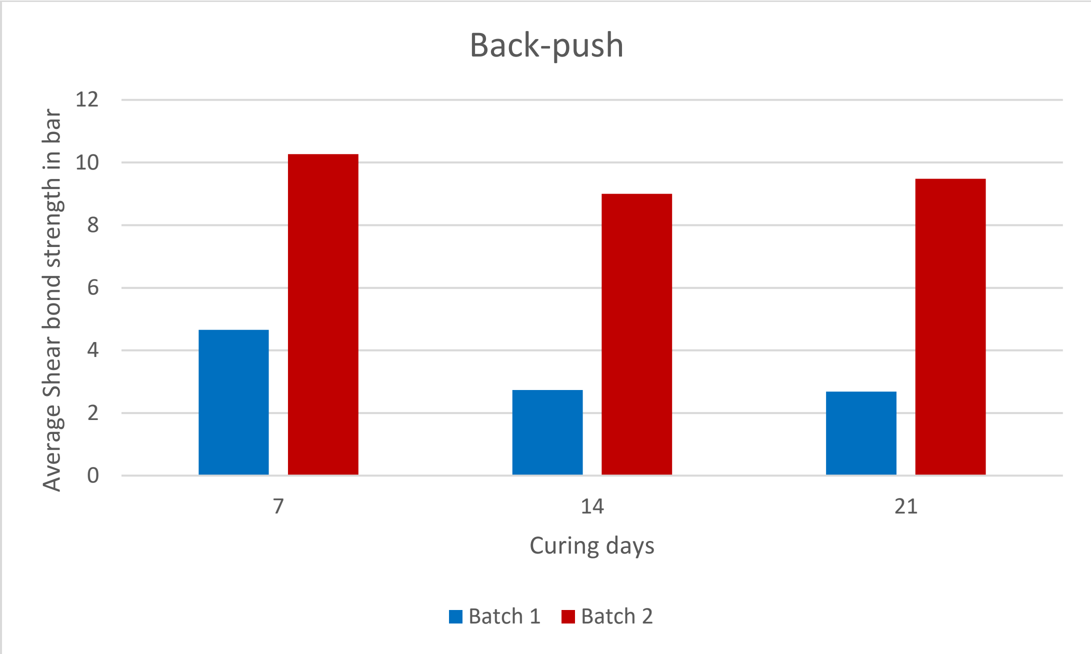

Figure 32: Average shear bond strength back-push

We can clearly see in Figure 31 and 32 that Batch 2 has a considerably greater shear bond strength. This corresponds well with our other results, and it answers our question clearly that we indeed need more force to move the expansive cement through the pipes than the Neat Class-G cement. We calculate from Table 14 that Batch 2 on average has approximately 290% higher shear bond strength than batch 1 on front-push, and 300% higher shear bond strength on back-push.

Calculation Front-Push: (Using values from Table 14)

Day 7 in percent: $\frac{28.27}{11.36} * 100\%$ = 248.9%

Day 14 in percent: $\frac{25.30}{9.14} * 100\%$ = 276.8%

Day 21 in percent: $\frac{21.97}{6.41} * 100\%$ = 342.7%

On average: $\frac{248.9\%+276.8\%+342.7\%}{3}$ = 289.5%

Same procedure for back-push gives result: 301.2%

To gain a deeper understanding of the bonding mechanism between the cement and the casing wall, it is necessary to closely examine the interlocking forces that occur between these two materials. While this factor has not been extensively discussed thus far, studying the interlock force can provide further insight into the experimental results. Schematic drawing showing how the interlock force is applied.

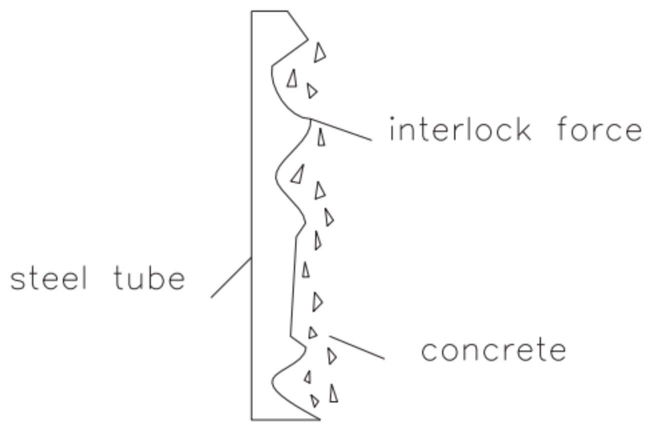

Figure 33: Interlock force

Interlock force refers to the mechanical interlocking of rough surfaces of two materials in contact with each other. When two materials with rough surfaces are pressed together, the asperities of one surface deform and interlock with the asperities of the other surface, creating an interlocking force that holds the two materials together. A visual representation of this is shown in Figure 33.

In the context of cementing in the petroleum industry, interlock force is important for achieving a strong bond between the casing and the cement. When the cement is pumped into the annulus between the casing and the wellbore, it fills the voids and crevices in the rough surface of the casing, creating a mechanical interlocking force that holds the cement and casing together. The interlock force can provide additional bond strength in addition to the chemical bond between the cement and the casing (Chen *et al*, 2017).

Axial bond-slip is a term used to describe the relative movement between two adjacent sections of a cement sheath in a wellbore. It refers to the degree of bonding and sliding resistance between the cement and the steel casing or the formation. During the drilling and production process, the cement sheath may undergo various mechanical and environmental stresses, which can cause bond failure and result in unwanted fluid or gas migration. Therefore, axial bond-slip is an important factor to consider in designing and evaluating the performance of the cement sheath. By measuring and analyzing axial bond-slip, engineers can better understand the integrity and stability of the wellbore and optimize cementing operations to prevent potential issues such as leaks and formation damage.

Typical axial bond-slip curves based on test results; These figures and the explanations are obtained from ''*Bond-slip behaviour of concrete-filled stainless steel circular hollow section tubes*'' (Chen *et al*, 2017).

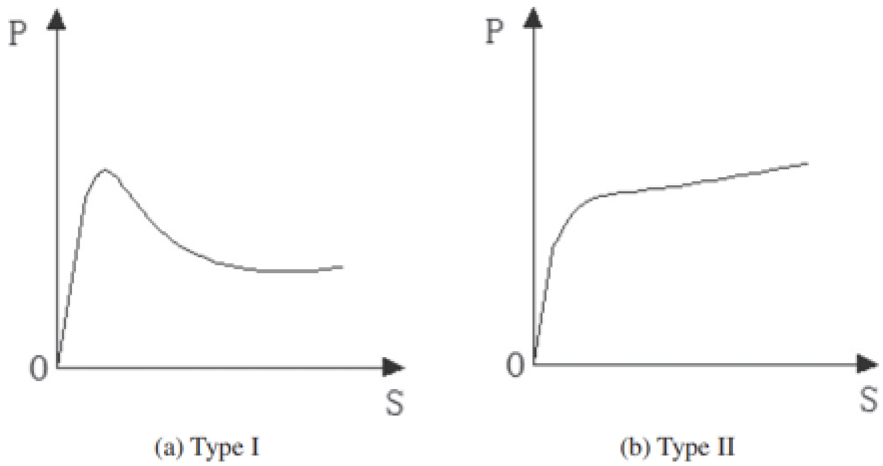

Figure 34: Typical axial load curves

The interface friction force can be reduced by increasing the resultant interlock force and adhesive force of the interface elements. If these forces exceed the initial interface friction force, a peak point will be observed in the testing curve (Type 1 Figure 34), followed by the post-ultimate stage. This type of testing curve typically occurs in specimens with a coarse inner surface of a stainless-steel tube. Conversely, if the resultant interlock force and adhesive force of the interface elements are smaller than the initial interface friction force, no clear peak point can be found in the testing curve (Type 2), and a knee point is formed instead, followed by a continuous increase in axial load. This type of testing curve generally occurs in specimens with a smooth inner surface of a stainless-steel tube. This matches great with our results and the front-pushes have all been of Type 1, while the back-pushes are similar to Type 2.

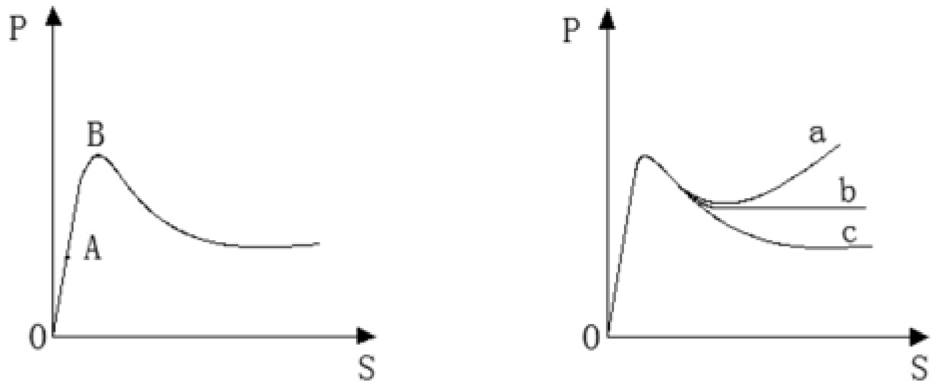

Figure 35: Typical axial load curves 2

The post-ultimate stage (after the peak point or the knee point in the testing curve) varies significantly for different specimens, depending on the degree of smoothness of the inner surface of the stainless-steel tube. If the degree of smoothness is significantly uneven, the interface friction force greatly increases with the increase of the bond-slip, resulting in a clear increasing post-ultimate stage, which we can see as curve ''a'' in Figure 35. However, if the degree of smoothness is even, the interface friction force greatly decreases with the increase of the bond-slip, resulting in a substantial dropping post-ultimate stage. Shown as curve ''c''. For specimens with a medium degree of smoothness, the post-ultimate stage of axial load versus bond-slip curves is located between the curves for the specimens with significantly uneven and even degrees of smoothness. This stage is somewhat dropped, followed by a comparatively flat portion (Chen *et al*, 2017).

To summarize the discussion regarding the push-out testing, a comparison plot was generated to consolidate the test results for each specimen across the entire time frame. This allows for a more comprehensive view of the development of the specimens over time, and the resulting plots were divided into individual specimens, each displaying the results of the three push-out tests conducted after 7, 14, and 21 days. However, the initial plots contained a significant amount of noise due to oscillations and stick-slip effects, which made combining them into a single plot challenging. Because of this, we wrote a script in Excel to reduce the noise in the graphs and plot them together.

We used the Analysis ToolPak Add-in with the exponential smoothing function to create the script. The script uses a damping factor that can be set to any level. We wanted very smooth thin lines, so we chose to put this damping factor at 0,98. The formula then creates values at each point using 0,02 times the actual point value and adds it together with 0,98 times the previous number smooth value. At the first number, it just uses the real value as there is no previous smooth value. The formula then looks like this:

Where: $\mathbf{L_t}$ = measured load $\boldsymbol{\alpha}$ = damping factor

$\mathbf{S_{t-1}}$ = Smooth load from the previous number

$\mathbf{S_t}$= Smooth load

$$\mathbf{S_t} = \mathbf{(1-\alpha) \cdot L_t + \alpha \cdot S_{t-1}}$$

The following graphical representations in figures 35-40 are highly informative as they facilitate the comparison of test results obtained at varying curing durations. In addition, these plots enable clear visualization of the evolution of the specimens' properties throughout the repeated push-out testing process. As mentioned, the reason for conducting repeated push-out testing is to evaluate the durability of the bond between the cement and casing over time. Therefore, it is important to compare the test results; these graphs are a good way of doing that.

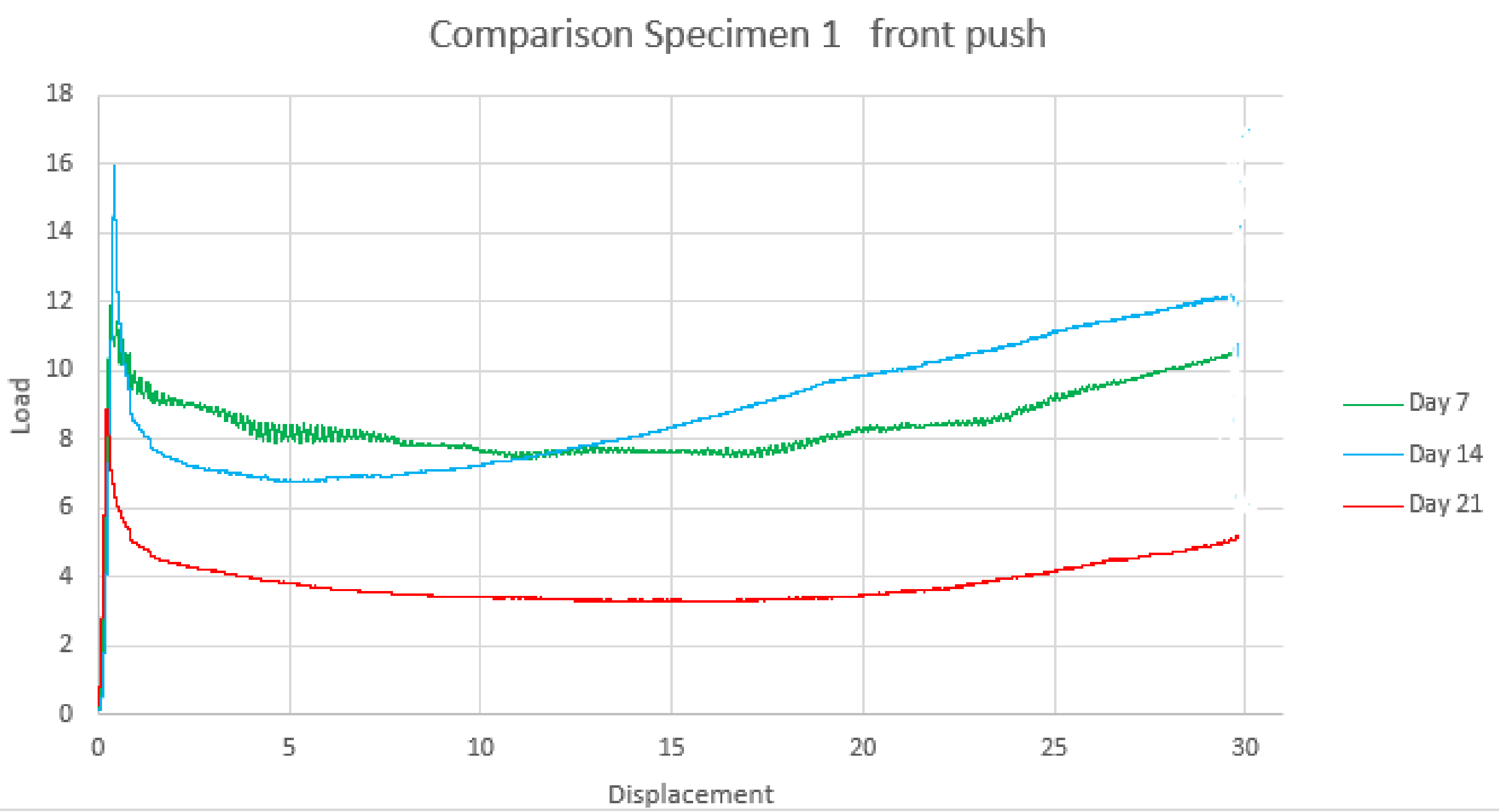

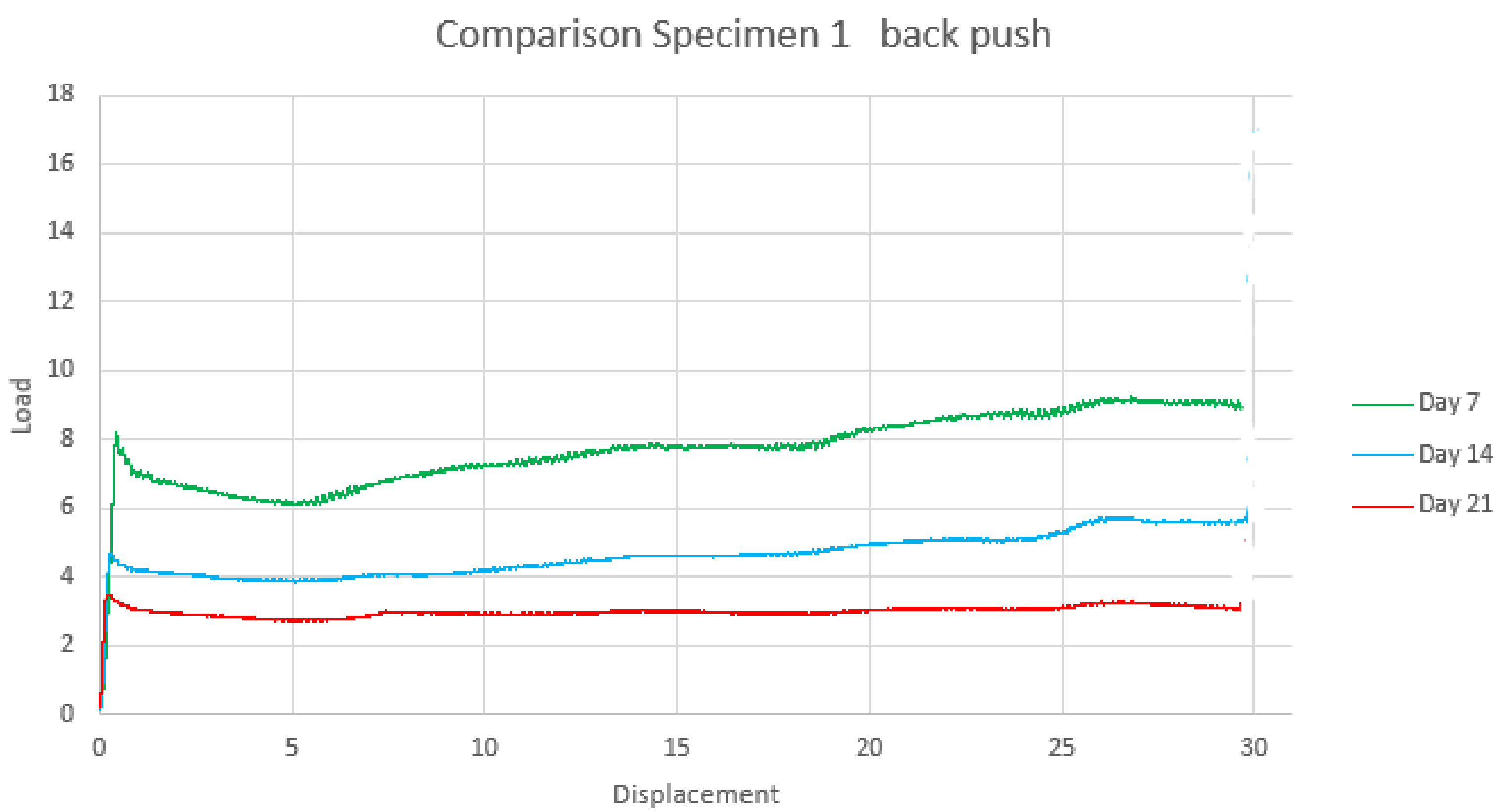

Figure 36: Comparison push-out specimen 1

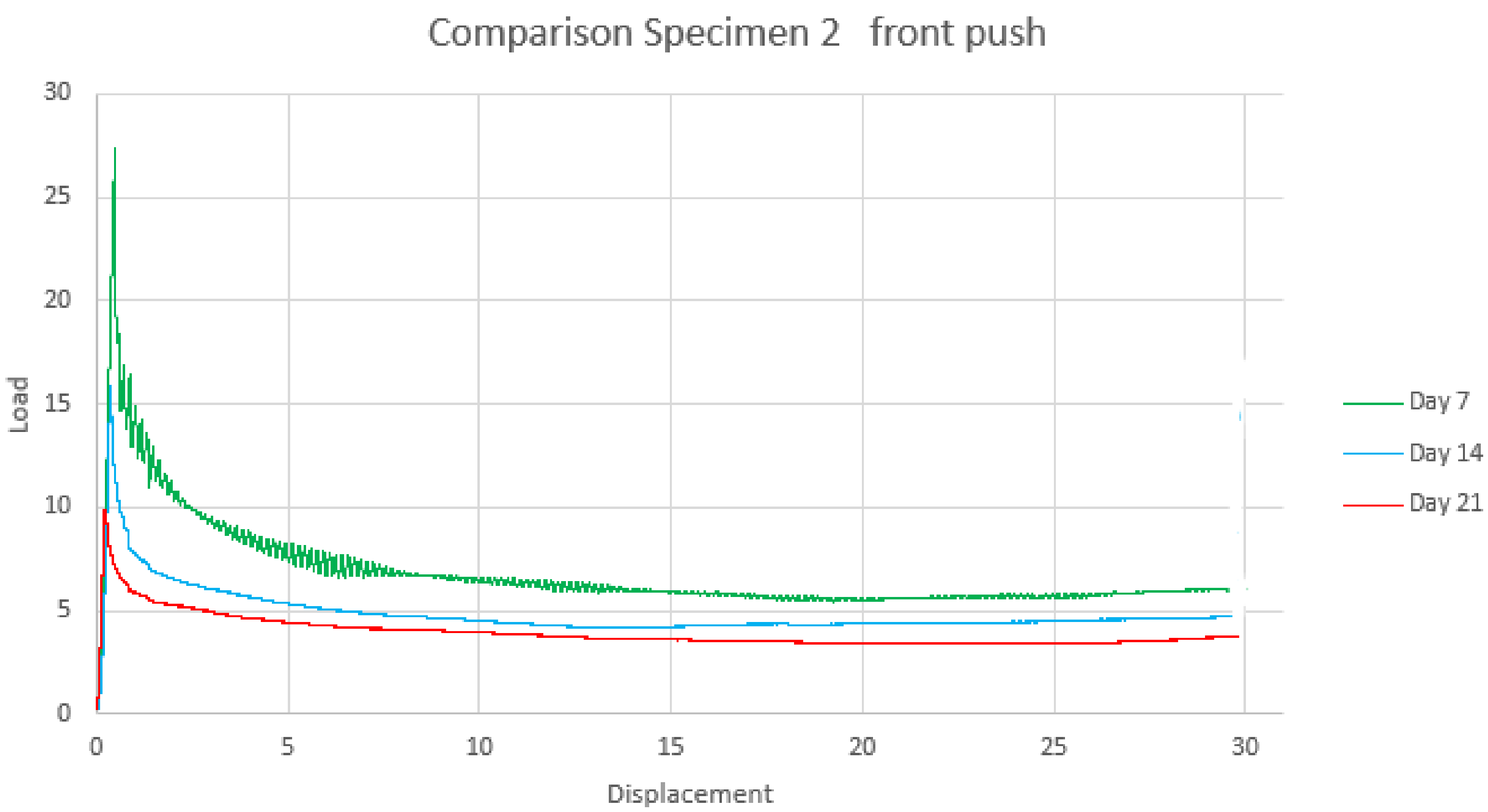

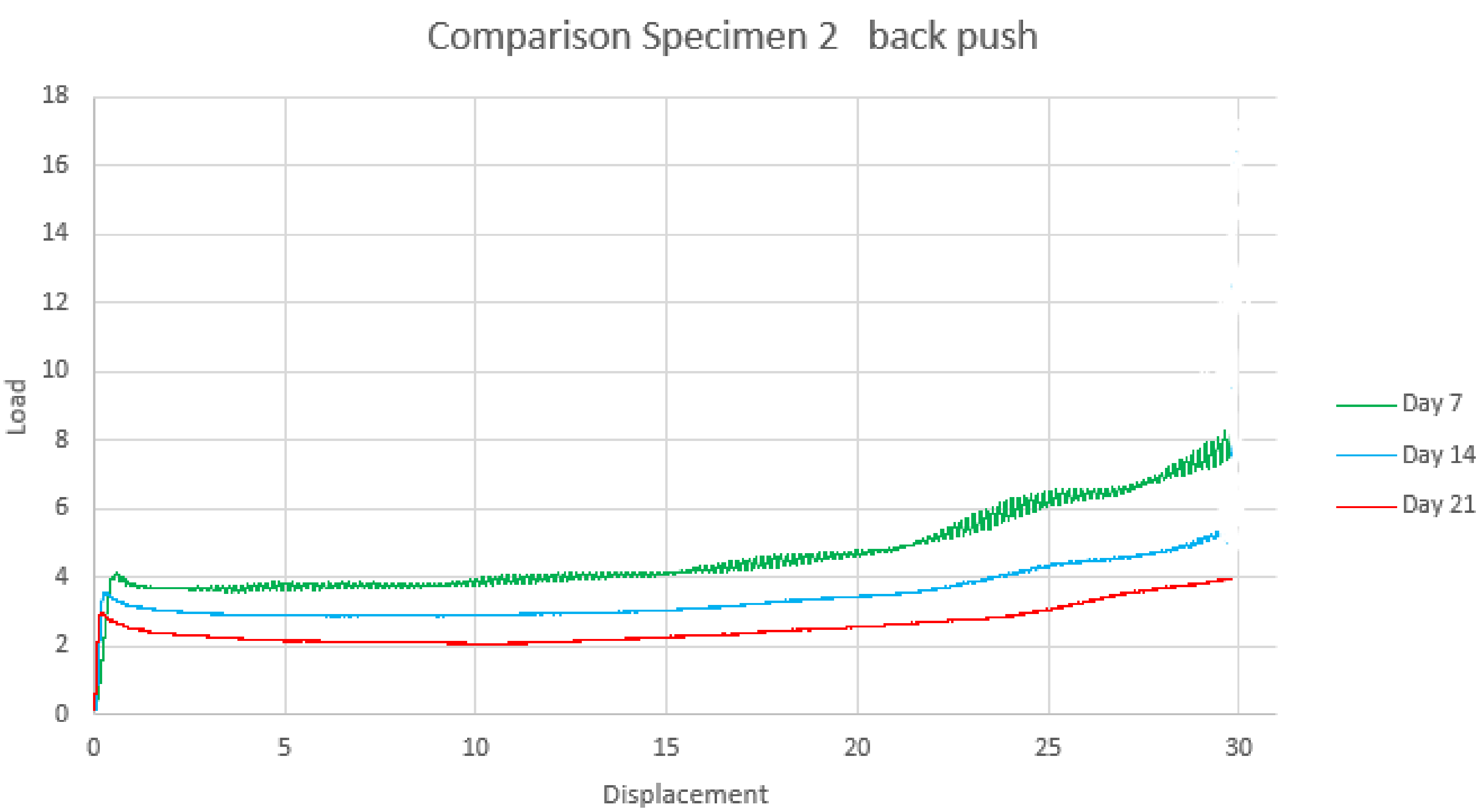

Figure 37: Comparison push-out specimen 2

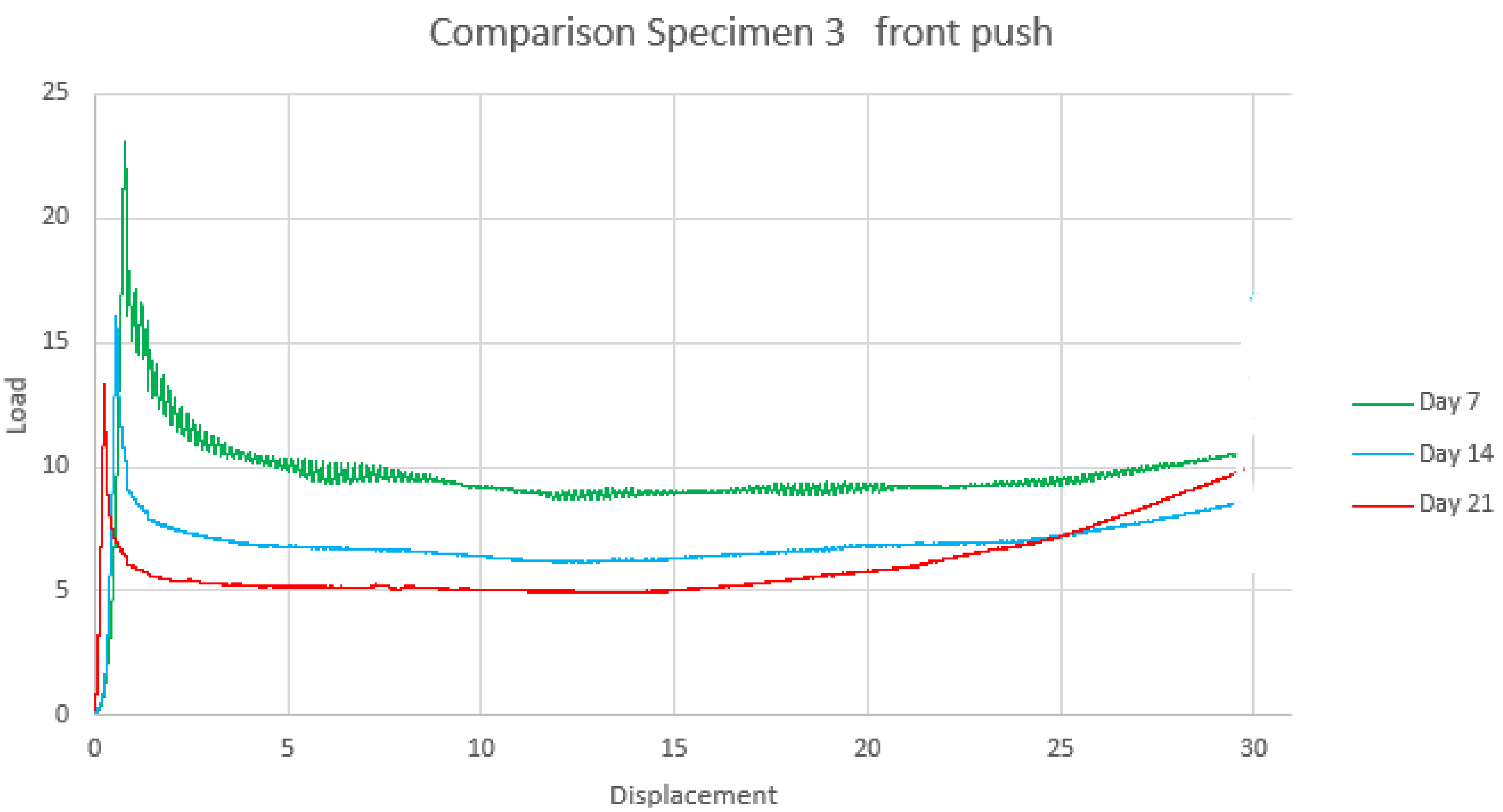

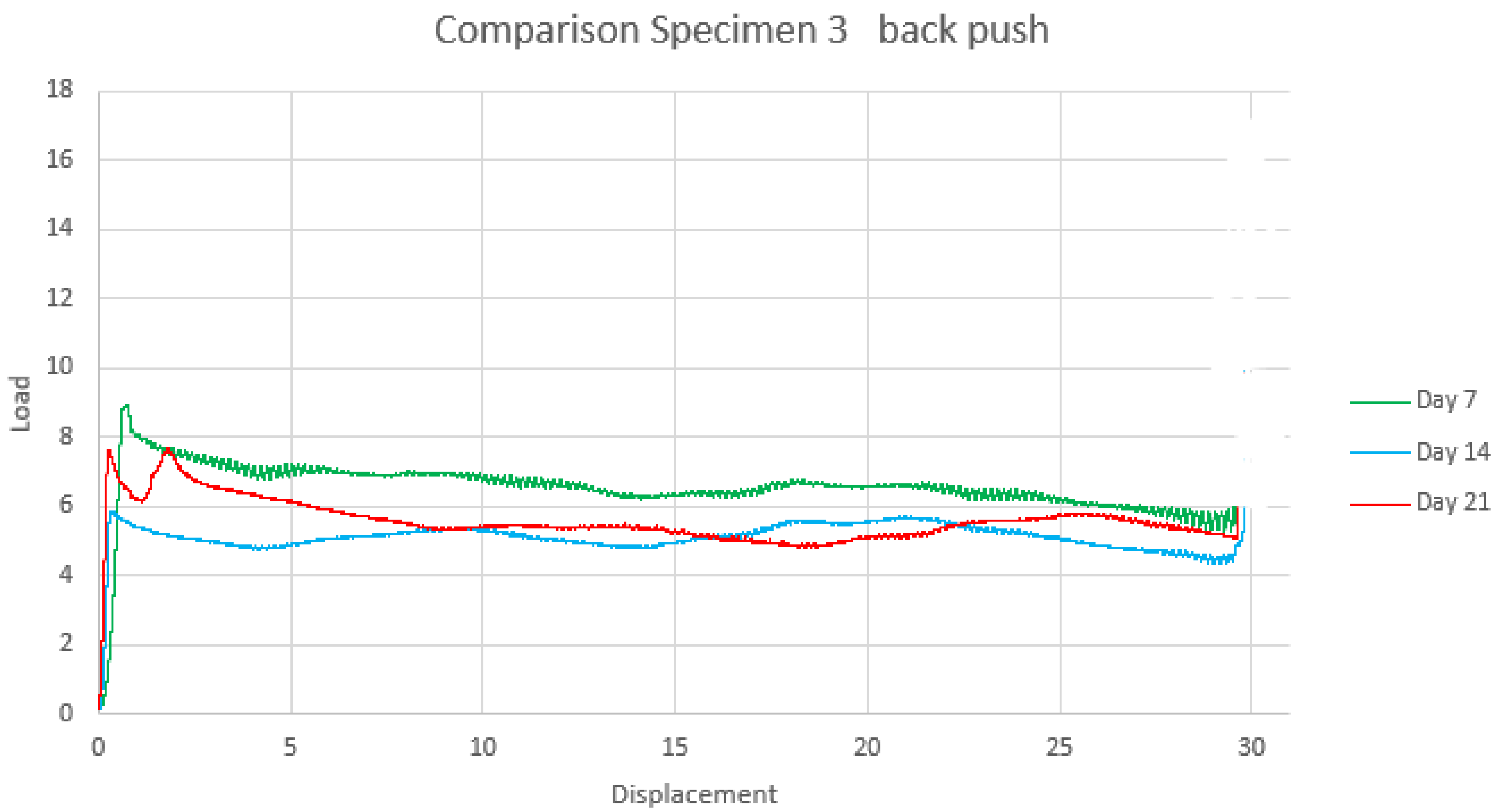

Figure 38: Comparison push-out specimen 3

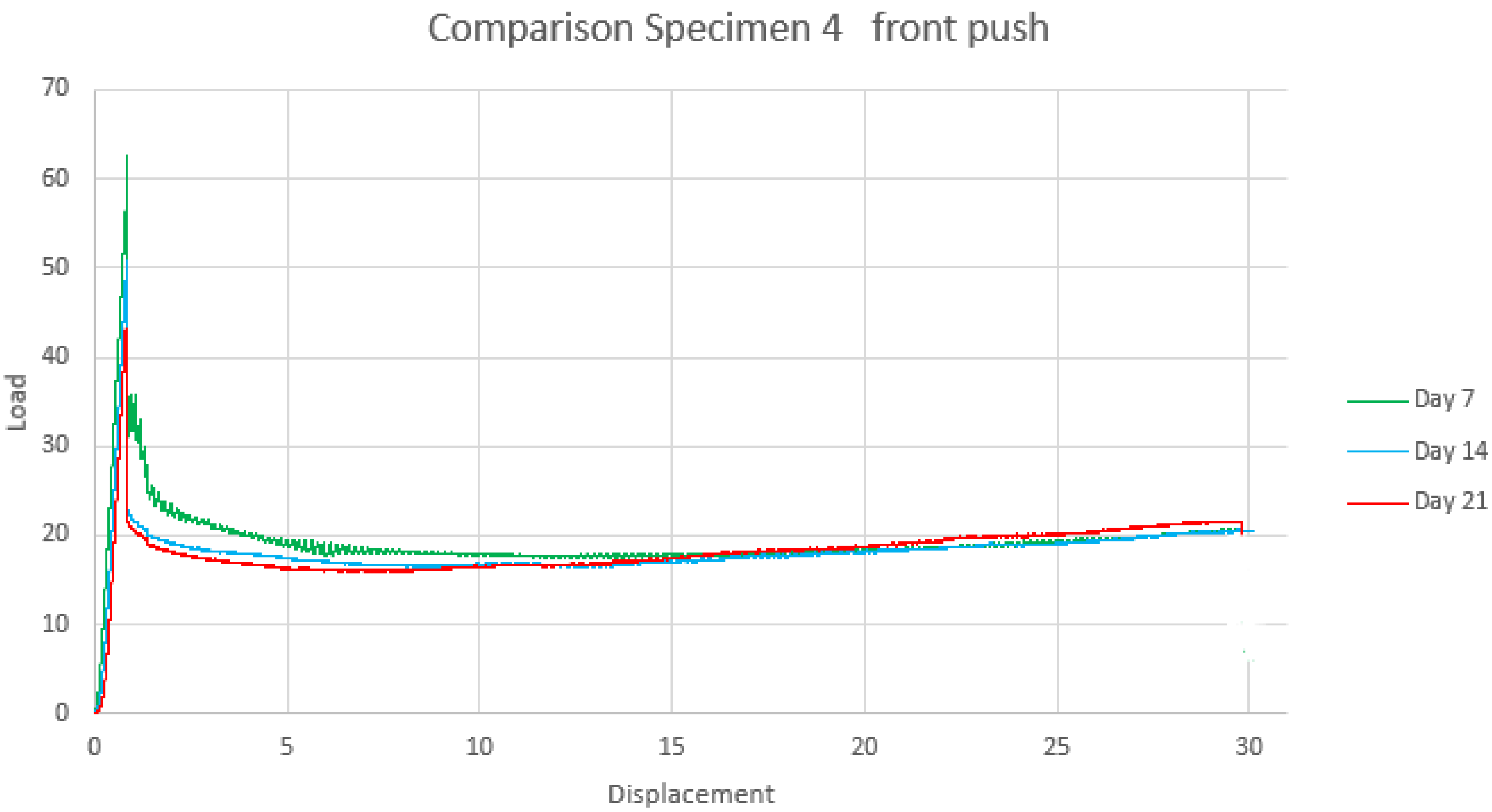

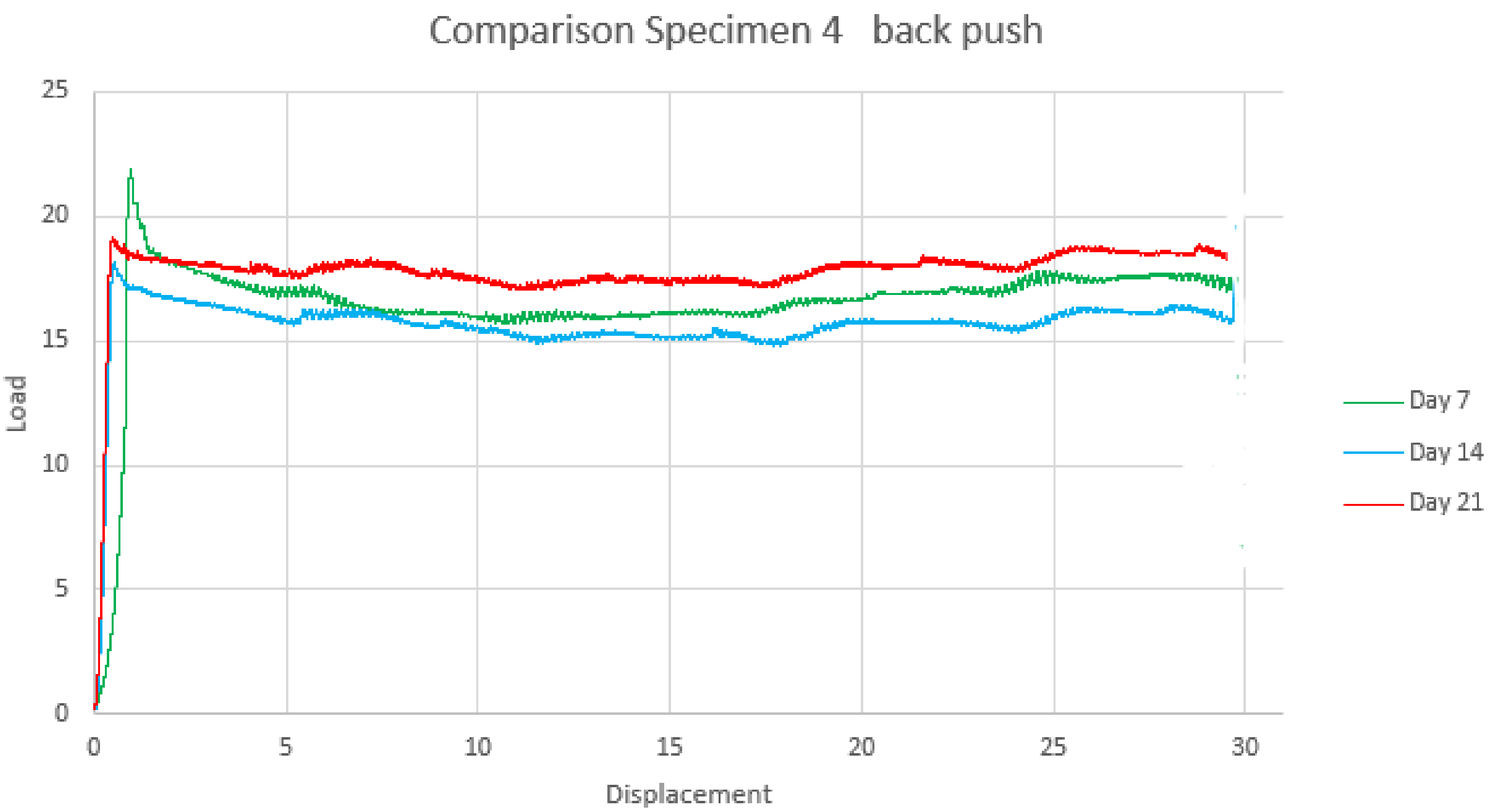

Figure 39: Comparison push-out specimen 4

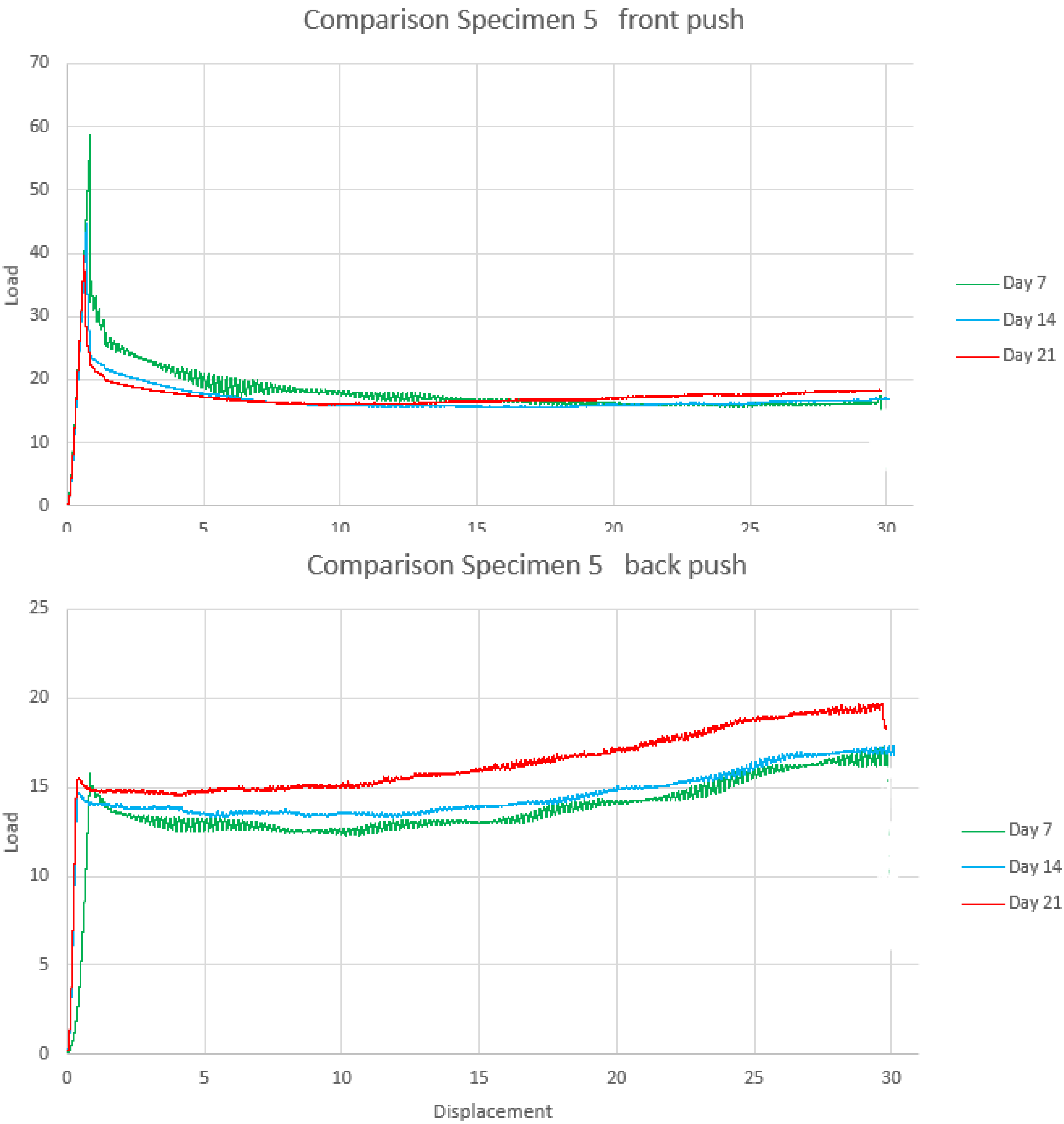

Figure 40: Comparison push-out specimen 5

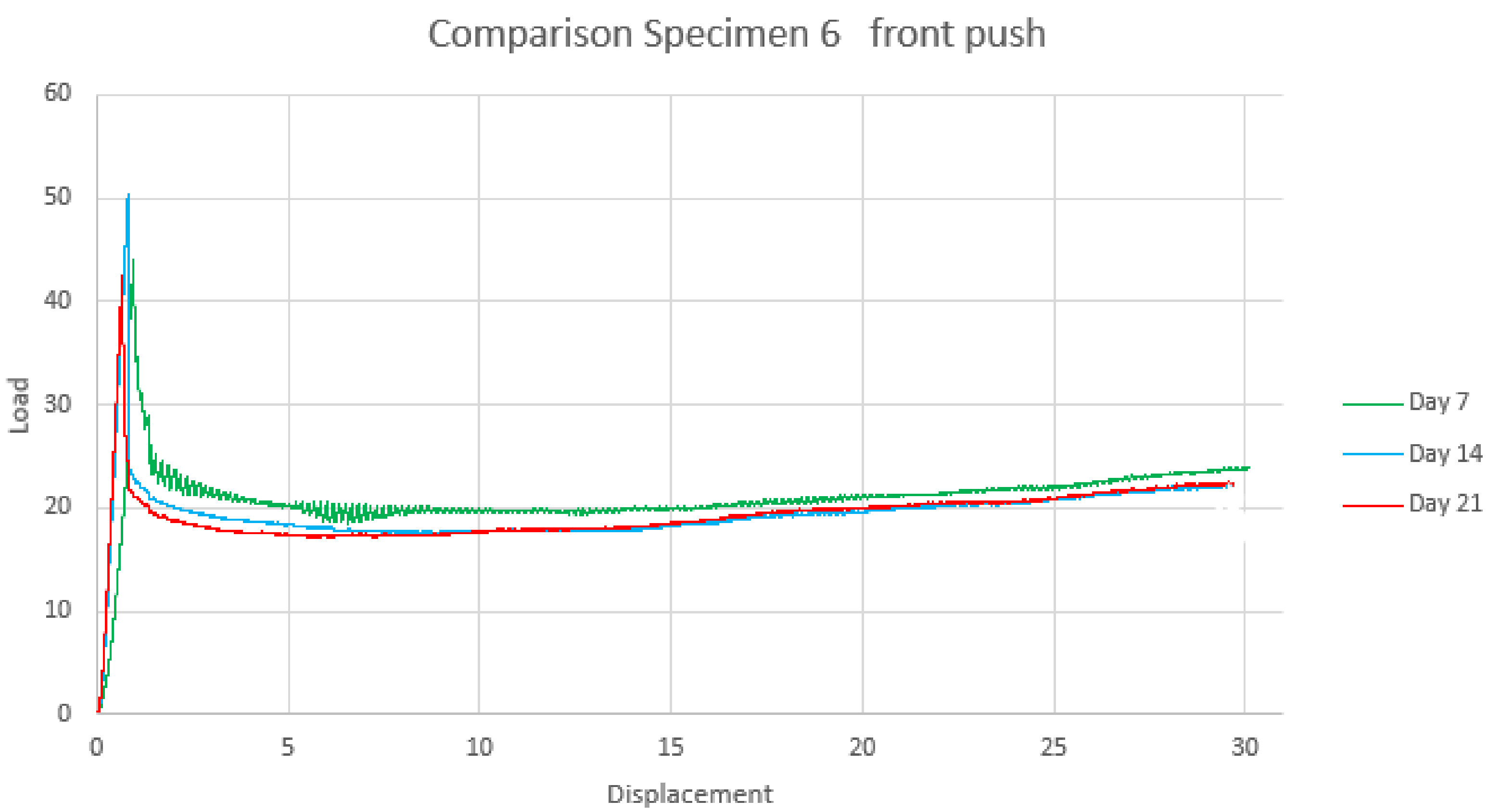

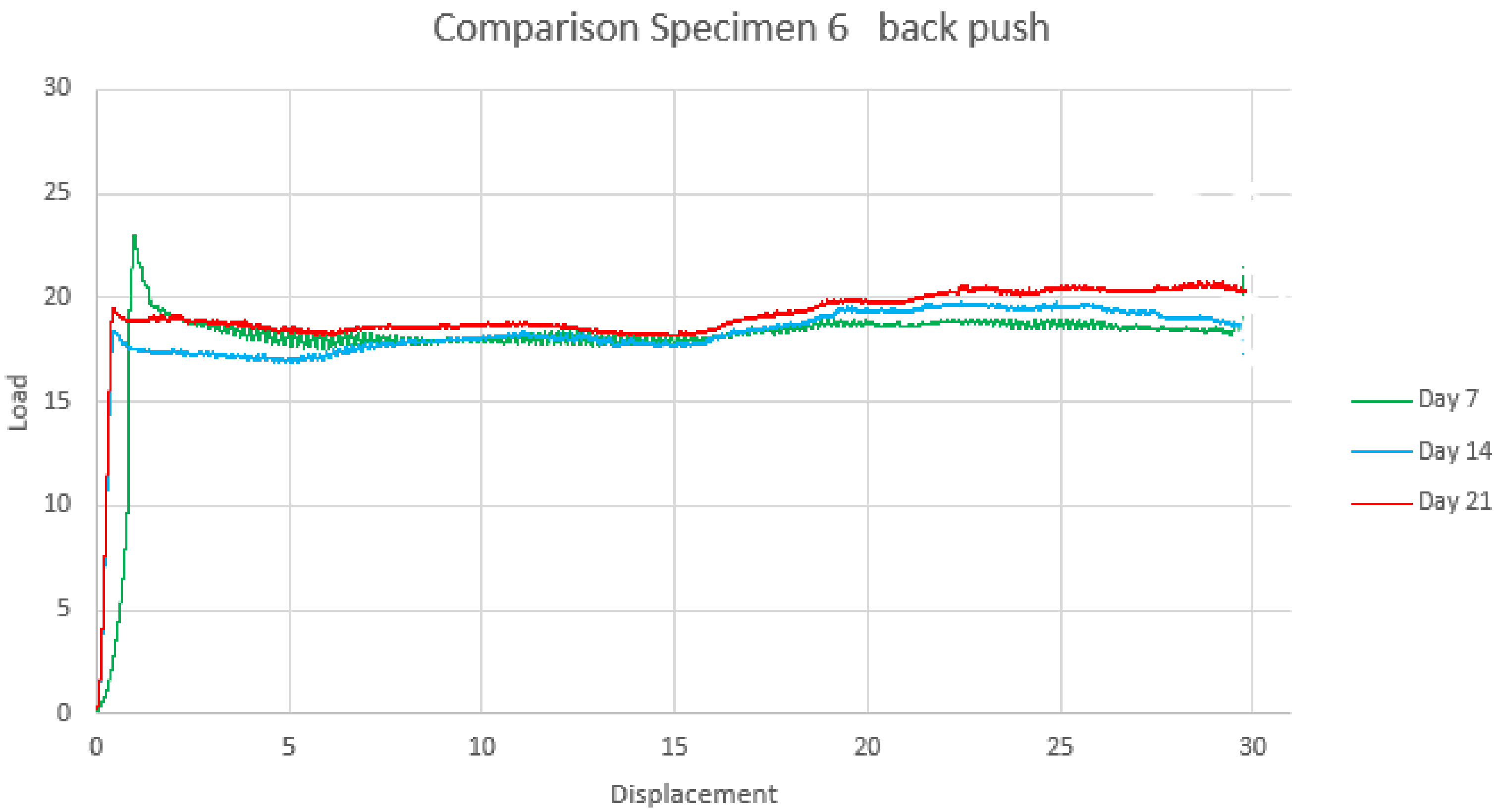

Figure 41: Comparison push-out specimen 6

7. Conclusion

Our goal for this thesis was to study the difference the expansive agent had on shear bond strength and expansion. Through our results and discussion, we conclude that:

- Addition of MicroBond gives a great increase in peak load and shear bond strength. Hence the load needed to push the expansive agent cement is a lot higher than the Neat Class-G cement.

- The difference between Neat Class-G and Halliburton blend in shear bond strength is approximately the same for both front- and back-push, with increases of 290% and 300%, respectively.

- Shear bond strength is the strongest on the first push of testing and then decreases for every push.

- The behavior of both slurries seems similar in terms of how the graphs are shaped for both front- and back-push.

- There is a clear increase in linear expansion when adding MicroBond. The average linear expansion was measured to be 0.170% for Neat Class-G cement, and 0.222% for the Halliburton blend.

- Neat Class-G cement had 95% of total linear expansion inside the first 24 hours. The Halliburton blend had a more spread-out expansion, with only 69 % in the first 24 hours.

- Measured a volumetric expansion of 0.761% on average over the entire test period using the volumetric expansion test.

- Our new experiment is a viable method to measure volumetric expansion with a good accuracy towards the results from the API-ring test.

- Using our results, we verified a mathematical relationship between linear expansion from the API ring and volumetric expansion from our experiment.

8. Figure sources

Figure Number	Owner	Copied from	Date of copy	Page Number
1	SLB	https://www.slb.com/resource-library/oilfield-review/defining-series/defining-cementing	25/02/23	11
2	SLB	https://www.slb.com/resource-library/oilfield-review/defining-series/defining-cementing	25/02/23	12
3	SLB	*«Well cementing, Second edition»* - Page 3 (Nelson and Guillot, 2006)	10/03/23	13
6	API	API recommended Practice 10B-5 Page 3	04/02/23	21
7	API	API recommended Practice 10B-5 Page 8	04/02/23	22
13	3B Scientific	https://www.3bscientific.com/us/baseline-volumetric-measuring-device-hand-set-3x5x11-w72247-baseline-12-3500,p_911_29150.html	09/04/23	32
22	Docsity	https://www.docsity.com/en/stick-slip-behavior-seismology-lecture-slides/377729/	25/03/23	45
33	Elsevier	"Bond-slip behaviour of concrete-filled stainless steel circular hollow section tubes" - (Chen *et al,* 2017) Page 259	25/03/23	56
34	Elsevier	"Bond-slip behaviour of concrete-filled stainless steel circular hollow section tubes" - (Chen *et al,* 2017) Page 258	15/04/23	57
35	Elsevier	"Bond-slip behaviour of concrete-filled stainless steel circular hollow section tubes" - (Chen *et al,* 2017) Page 258	15/04/23	58

9. References

3B Scientific. (2023). *Baseline volumetric measuring device, hand set, 3x5x11"*. Retrieved from 3B Scientific: https://www.3bscientific.com/us/baseline-volumetric-measuring-device-hand-set-3x5x11-w72247-baseline-12-3500,p_911_29150.html

Aïtcin, P., & R.J, F. (2016). *Science and Technology of Concrete Admixtures.* Woodhead Publishing. Retrieved from https://doi.org/10.1016/C2015-0-00150-2

American Petroleum Institute. (2005, Rev 2015, April). Recommended Practice on Determination of Shrinkage and Expansion of Well Cement formulations at atmospheric pressure. *Recommended practice 10B-5, first edition*. USA: API.

American Petroleum Institute. (2013, April). Recommended Practice for Testing. *API Recommended practice 10B-2, second edition*. USA: API.

Backe, K. R., Skalle, P., O.B, L., Lyomov, S., H, J., & J, S. (1998, September). *Shrinkage of Oil Well Cement Slurries*. Retrieved from NTNU: http://www.ipt.ntnu.no/~pskalle/files/TechnicalPapers/13_shrinkage.pdf

Cadix, A., & James, S. (2021). Chapter 5 - Cementing additives. In Q. Wang, *Fluid Chemistry, Drilling and Completion* (pp. 187-254). Gulf Professional Publishing. Retrieved from https://doi.org/10.1016/B978-0-12-822721-3.00008-3

Chen, Y., Feng, R., Shao, Y., & Zhang, X. (2017). *Bond-slip behaviour of concrete-filled stainless steel circular hollow section tubes.* Journal of Constructional Steel Research, Volume 130, Pages 248-263. Retrieved from https://doi.org/10.1016/j.jcsr.2016.12.012

del Strother, P. (2019). 2 - Manufacture of Portland Cement. In P. C. Hewlett, & M. Liska, *Lea's Chemistry of Cement and Concrete* (pp. 31-56). Butterworth-Heinemann. Retrieved from https://doi.org/10.1016/C2013-0-19325-7

Dyckerhoff. (2021, April 29). *Dyckerhoff Well Cement Class G*. Retrieved from Dyckerhoff: https://www.dyckerhoff.com/documents/209745/1442411/Class+G_Lengerich.pdf

Guillot, D., & Nelson, E. B. (2006). *Well Cementing second edition.* Texas: Schlumberger.

Gundersen, N., & Lundberg, N. H. (2023, Januar 26). *Petroleumsutvinning*. Retrieved from Store Norske Leksikon: https://snl.no/petroleumsutvinning

Halliburton. (1996, January). *Expansive Additives*. Retrieved from Oildoc: http://oildoc.ir/wp-content/uploads/2019/02/SECT_17_Expansive_Additives.pdf

Liska, M., Wilson, A., & Bensted, J. (2019). 13 - Special Cements. In P. C. Hewlett, & M. Liska, *Lea's Chemistry of Cement and Concrete* (pp. 585-640). Butterworth-Heinemann. Retrieved from https://doi.org/10.1016/C2013-0-19325-7

PCA. (n.d.). *How Cement is Made*. Retrieved from cement.org: https://www.cement.org/cement-concrete/how-cement-is-made

Petro Drilling Mining oil Co. (n.d.). *Oil Well Cement Class G*. Retrieved from Petrodmo: https://www.petrodmo.com/products/oil-well-cement-class-g

PetroWiki. (2015, June 25). *Cement bond logs*. Retrieved from PetroWiki: https://petrowiki.spe.org/Cement_bond_logs

Rahman, S. H., Irawan, S., Shafiq, N., & Rajeswary, R. (2020, February). Investigating the expansion characteristics of geopolymer cement samples in a water bath and compared with the expansion of ASTM Class-G cement. *Heliyon, 6*(2). Retrieved from https://doi.org/10.1016/j.heliyon.2020.e03478

Rudawska, A. (2019). *Surface Treatment in Bonding Technology.* Lubin: Academic Press. Retrieved from https://doi.org/10.1016/C2018-0-01281-5

Sandal, R., Sharma, R., & Ren, W. (2020, January 1). Bond-slip characterization of the interfacial transition zone of cement concrete and granite rock using push-out test. *Materials Today: Proceedings, 32*, 951-954. Retrieved from https://doi.org/10.1016/j.matpr.2020.05.090

Schlumberger. (2012, January 1). The Defining Series: Well Cementing Fundamentals. (E. B. Nelson, Ed.) *Oilfield Review Summer 2012, 24*. Retrieved from Slb: https://www.slb.com/resource-library/oilfield-review/defining-series/defining-cementing

Thue, J. V. (2019, July 16). *Betong*. Retrieved from Store Norske Leksikon: https://snl.no/betong

Veyssière, P., Kramer, E., Mahajan, S., Ilschner, B., Cahn, R., Buschow, J., & Flemings, M. (2001). *Encyclopedia of Materials: Science and Technology.* Pergamon. Retrieved from https://www.sciencedirect.com/referencework/9780080431529/encyclopedia-of-materials-science-and-technology#book-description

Wise, J., Al Dushaishi, M., Bocanegra-Yanez, J., Lee, H. P., & Hunt, S. L. (2023, june). Experimental analysis of Wellbore cement-steel bond mechanics. *Geoenergy Science and Engineering, 225*. Retrieved from https://doi.org/10.1016/j.geoen.2023.211709

Xu, C., Chengkui, H., Decheng, J., & Yuancheng, S. (2009, January). Push-out test of pre-stressing concrete filled circular steel tube columns by means of expansive cement. *Construction and Building Materials, 23*(1), 491-497. Retrieved from https://doi.org/10.1016/j.conbuildmat.2007.10.021

Årtun, T. (2023, January 24). *Sement*. Retrieved from Store Norske Leksikon: https://snl.no/sement